

Our greatest glory is not in never falling, but in rising every time we fall

He who understands is no better than he who appreciates and he who appreciates
is no better than he who enjoys

- Confucius

University of Alberta

Acid Labile Surfactants Containing Ketal-Linkage in Micellar Electrokinetic
Chromatography and Electrospray Ionization Mass Spectrometry

by

Bob Stanley

A thesis submitted to the Faculty of Graduate Studies and Research
in partial fulfillment of the requirements for the degree of

Master of Science

Department of Chemistry

©Bob Stanley

Fall 2012

Edmonton, Alberta

Permission is hereby granted to the University of Alberta Libraries to reproduce single copies of this thesis and to lend or sell such copies for private, scholarly or scientific research purposes only. Where the thesis is converted to, or otherwise made available in digital form, the University of Alberta will advise potential users of the thesis of these terms.

The author reserves all other publication and other rights in association with the copyright in the thesis and, except as herein before provided, neither the thesis nor any substantial portion thereof may be printed or otherwise reproduced in any material form whatsoever without the author's prior written permission.

~ ~ ~

This thesis is dedicated to my parents and significant other

~ ~ ~

ABSTRACT

The combination of micellar electrokinetic chromatography (MEKC) with electrospray ionization mass spectrometry (ESI-MS) would yield a very powerful analytical technique. However, hyphenating both techniques is not easy. Sodium 4-[(2-methyl-2-undecyl-1,3-dioxolan-4-yl) methoxy]-1-propane sulfonate (ALS) and sodium 2,2-Bis(hexyloxy)propyl sulphate (OALS) are possible solutions to link MEKC with ESI-MS. They are surfactants that are hydrolyzable under acidic condition. Their hydrolysis products are compatible with ESI-MS. They can be utilized as pseudostationary phases to perform a separation and then acid-hydrolyzed before being introduced into the ESI-MS. Both surfactants are compared with sodium dodecyl sulphate (SDS). ALS and OALS offer different selectivity than SDS. In term of mobility, ALS has a slower mobility than SDS. OALS has a greater mobility than SDS. ALS contains a cyclic ketal while OALS contains an acyclic ketal. OALS hydrolyzes much faster than ALS. The hydrolysis can be slowed down by lowering the temperature and vice versa.

ACKNOWLEDGEMENT

First and foremost, I would like to thank my supervisor, Dr. Charles A. Lucy for his mentorship and patience over the course of my graduate study. When I first started this research project, it was daunting. But he patiently guided me through the project. He also provided me with numerous guidance and answers whenever I was stuck in the project. He did not only teach me the chemistry, but he also taught me numerous invaluable transferrable skills over the past 2.5 years. The research presented in this thesis would not have been possible if not for his knowledge and supervision. I could not have picked a better and more understanding supervisor.

Next is the group of people I shared the lab and office with, the Lucy Group. Thank you for the numerous comedic and scientific conversations. I would like to give special thanks to Lei Pei for being a supportive friend and confidant. I am thankful to have met someone like her I am proud to call one of my best friends. Mahmoud Bahnasy, Ping Jiang and Wu Di also need to be specially mentioned for entertaining me most of the times. I could not have asked for a better group of people to share an office space with. W3-18 is always full of laughter because of you three. I would also like to thank Farooq Wahab for the benefit of his opinion and very informative discussion.

The financial support of the Natural Sciences and Research Council of Canada and the Department of Chemistry at the University of Alberta is gratefully acknowledged.

I would also like to acknowledge Dr. Kingsley K. Donkor of Thompson Rivers University in Kamloops, British Columbia. He has taught me very well and I am extremely fortunate to have him as a mentor in my undergraduate years. I would not have even thought of graduate school if not for his advice and encouragement.

Thank you to my parents, Samas and Fransiska for their love and endless support. Everything that I am today is a result of their strict, discipline and loving education when I was young. Looking back, I hated the discipline and corporal punishment, but I know they did it out of love and to prepare me for the world.

The acknowledgement is not complete if I do not thank the best roommate a guy could have asked for, Nikolai A. Sinkov. Thank you for your friendship, scientific discussion and helping to pay the rent. I want to thank Nikolai's group and supervisor (The Harynuk Group and Dr. James Harynuk) for adopting me into their group.

Lastly, I am infinitely grateful to my significant other Shani A. Linarta for her support, encouragement and love especially during the course of writing this thesis. Thank you for all the encouragement and help yayang. I love you.

TABLE OF CONTENTS

CHAPTER 1 INTRODUCTION	1
1.1 CAPILLARY ELECTROPHORESIS.....	1
1.2 MICELLAR ELECTROKINETIC CHROMATOGRAPHY	5
1.2.1 Principle of Micellar Electrokinetic Chromatography	5
1.2.2 Selectivity of the Pseudostationary Phase.....	10
1.2.3 Mobility of the Pseudostationary Phase.....	11
1.2.3.1 Single-marker Method	12
1.2.3.2 Homologous Series Method.....	13
1.3 ELECTROSPRAY IONIZATION MASS SPECTROMETRY	15
1.3.1 Brief history of electrospray ionization mass spectrometry	15
1.3.2 Ion Formation Mechanism	16
1.3.3 Ion Suppression in ESI-MS by Surfactant	19
1.4 CLEAVABLE SURFACTANTS	22
1.4.1 Acid-labile Surfactant	22
1.4.2 Surfactants with an Acid-labile Ketal-linkage	23
1.5 OUTLINE OF THESIS	24
1.6 REFERENCES.....	26

CHAPTER 2 MICELLAR ELECTROKINETIC CHROMATOGRAPHY WITH ACID LABILE SURFACTANT.....	31
2.1 INTRODUCTION.....	31
2.2 EXPERIMENTAL.....	34
2.2.1 Materials and Reagents.....	34
2.2.2 Synthesis of ALS.....	34
2.2.3 Instrumentation.....	36
2.3 RESULTS AND DISCUSSION.....	37
2.3.1 Comparison of MEKC with ALS and SDS.....	37
2.3.2 Stability of ALS Under Acidic Conditions.....	41
2.3.3 Mobility and Selectivity of ALS.....	42
2.3.4 Cleavage Rate of ALS and Compatibility with ESI-MS.....	46
2.5 REFERENCES.....	52
CHAPTER 3 MICELLAR ELECTROKINETIC CHROMATOGRAPHY AND ELECTROSPRAY IONIZATION MASS SPECTROMETRY WITH AN ACYCLIC KETAL-CONTAINING SURFACTANT.....	56
3.1 INTRODUCTION.....	56
3.2 EXPERIMENTAL.....	58
3.2.1 Materials and Reagents.....	58

3.2.2	Synthesis of OALS	59
3.2.3	Instrumentation	61
3.3	RESULTS AND DISCUSSION	62
3.3.1	Mobility and Selectivity of OALS	62
3.3.2	Cleavage Rate and Compatibility with ESI-MS	67
3.3.3	Controlling the Hydrolysis Rate of OALS with Temperature	72
3.4	CONCLUDING REMARKS	78
3.5	REFERENCES.....	80
CHAPTER 4	83
Section 4.1	GENERAL DISCUSSION AND CONCLUSIONS.....	83
Section 4.2	FUTURE WORK.....	85
4.3	REFERENCES.....	86

LIST OF TABLES

Table 2-1	Comparison of efficiency, repeatability and retention factor (k') between SDS and ALS as a pseudostationary phase.....	40
-----------	--	----

LIST OF FIGURES

Figure 1-1	Schematic diagram of a CE instrument in normal polarity mode.....	2
Figure 1-2	Structure of surfactant.....	6
Figure 1-3	Equilibrium between surfactant monomer and its micelle above the CMC.....	7
Figure 1-4	Schematic illustration of the principle of MEKC with anionic micelle and stronger EOF under normal polarity.....	9
Figure 1-5	Alkylphenone homologous series (acetophenone – hexanophenone).....	13
Figure 1-6	Positive deviation of plot of $\log k'$ vs. carbon number of alkylphenones. The pseudostationary phase is an acid-labile surfactant.....	15
Figure 1-7	Schematic of ion formation in ESI-MS.....	17
Figure 1-8	Surfactant monomers at the liquid-air interface inside a droplet. The hydrophobic tail is oriented towards the gas phase while the hydrophilic head is anchored in the inner of the droplet.....	20
Figure 1-9	Equilibrium between a ketal and its corresponding ketone.....	23
Figure 1-10	Structures of ALS (cyclic ketal) and OALS (acyclic ketal).....	24
Figure 2-1	Acid hydrolysis of ALS into its less surface-active products.....	33

Figure 2-2	Precursor of ALS (HMUD) synthesis monitoring. The rate of disappearance of the carbonyl peak of 2-tridecanone at 1720 cm ⁻¹ IR (neat film).....	35
Figure 2-3	Reaction scheme for synthesis of HMUD and ALS.....	36
Figure 2-4	Separation of six model analytes using ALS as a pseudostationary phase: benzene, toluene, butyrophenone, 2-naphthol, naphthalene, hexanophenone. Conditions: EOF marker, methanol; detection, 214 nm; applied voltage, 15 kV; BGE, 50 mM NaH ₂ PO ₄ , 100 mM borate, 30 mM ALS, pH 7.04; capillary (50 μm ID) total length, 51.5 cm; effective length, 41.5 cm.....	39
Figure 2-5	Stability plot of ALS for 60 hours. Conditions: Analyte, benzyl alcohol; EOF marker, methanol; detection, 214 nm; applied voltage, 15 kV; BGE, 50 mM NaH ₂ PO ₄ , 100 mM sodium borate, 30 mM ALS, pH 4.00. Capillary: 50 μm ID; total length, 51.5 cm; effective length, 41.5 cm.....	42

Figure 2-6 Log k' of eleven analytes using ALS and SDS as pseudostationary phase. □ = hydrogen bond donating (resorcinol, phenol, benzyl alcohol, 2-naphthol), $R^2= 0.74$; ■ = hydrogen bond acceptor (4-nitroaniline, butyrophenone, valerophenone, hexanophenone), $R^2= 0.88$; ▲ = non-hydrogen bonding (benzene, toluene, naphthalene), $R^2= 0.992$. Conditions: EOF marker, methanol; detection, 214 nm; applied voltage, 15 kV; BGE, 50 mM NaH_2PO_4 , 100 mM sodium borate, 30 mM ALS or SDS, pH 7.04.....46

Figure 2-7 Mass spectra of atenolol and ALS at 0 minute and 16 hours. Conditions: 475 μL of atenolol (25 mM in 0.5% formic acid) spiked with 25 μL of ALS (25 mM in deionized water). Conditions: negative mode; fragmentation energy, 80 V; solvent system, methanol. Atenolol peak is $[\text{M}+\text{FA}-\text{H}]^-$. ALS peak is $[\text{M}]^-$48

Figure 2-8 Mass spectrum of atenolol and SDS at 16 hours. Conditions: 475 μL of atenolol (25 mM in 0.5% formic acid) spiked with 25 μL of SDS (25 mM in deionized water). Conditions: negative mode; fragmentation energy, 80 V; solvent system, methanol. Atenolol peak is $[\text{M}+\text{FA}-\text{H}]^-$. SDS peak is $[\text{M}]^-$48

Figure 2-9	Ratio of ALS/atenolol ESI-MS signal intensity over a period of 16 hours in H ₂ O. Conditions: 475 μL of atenolol (25 mM in 0.5% formic acid), pH 2.5, spiked with 25 μL of ALS (25 mM in deionized water). Conditions: fragmentation energy, 80 V; solvent system, methanol; Half-life of ALS, 48 min.....	49
Figure 2-10	Ratio of ALS/atenolol ESI-MS signal intensity over a period of 16 hours in 50% ACN/H ₂ O. Conditions: 475 μL of atenolol (25 mM in 50/50 ACN/0.5% formic acid), pH 2.5, spiked with 25 μL of ALS (25 mM in 50/50 ACN/0.5% formic acid). Conditions: fragmentation energy, 80 V; solvent system, methanol; Half-life of ALS, 170 min.....	50
Figure 3.1	Acid hydrolysis of OALS.....	58
Figure 3.2	Reaction scheme for the five-step synthesis of sodium 2,2-Bis(hexyloxy)propyl sulphate (OALS).....	60
Figure 3.3	High resolution ESI-MS mass spectrum of OALS, m/z = 339.1846 (predicted 339.1847).....	61
Figure 3.4	Plot of Log <i>k'</i> vs. Carbon number of the alkylphenones homologous series (acetophenone – valerophenone). Conditions: EOF marker, methanol; detection, 214 nm; applied voltage, 15 kV; BGE, 50 mM ammonium acetate, 30 mM OALS, pH 9.00.....	63

Figure 3.5 Log k' of thirteen analytes using OALS and SDS as pseudostationary phase. □ = hydrogen bond donor (resorcinol, phenol, aniline, 2-naphthol), $R^2= 0.93$; ■ = hydrogen bond acceptor (4-nitroaniline, acetophenone, propiophenone, butyrophenone, valerophenone), $R^2= 0.91$; ▲ = non-hydrogen bonding (benzene, toluene, naphthalene, 2-methylnaphthalene), $R^2= 0.992$. Analytes are listed in order of their retention with SDS. Conditions: EOF marker, methanol; detection, 214 nm; applied voltage, 15 kV; BGE, 50 mM ammonium acetate, 30 mM OALS or SDS, pH 9.00.....65

Figure 3.6 Electropherogram illustrating the difference in migration pattern of resorcinol and phenol when using OALS and SDS as pseudostationary phases. Condition: detection, 214 nm; applied voltage, 15 kV; BGE, 50 mM ammonium acetate, 30 mM OALS or SDS, pH 9.00; capillary (50 μm ID) total length, 51.5 cm; effective length, 41.5 cm.....66

Figure 3.7 Log k' of thirteen analytes using OALS and ALS as pseudostationary phase. □ = hydrogen bond donor (resorcinol, phenol, aniline, 2-naphthol), $R^2= 0.94$; ■ = hydrogen bond acceptor (4-nitroaniline, acetophenone, propiophenone, butyrophenone, valerophenone), $R^2= 0.98$; ▲ = non-hydrogen bonding (benzene, toluene, naphthalene, 2-methylnaphthalene), $R^2= 0.95$. Analytes are listed in order of their retention in ALS. Conditions: EOF marker, methanol; detection, 214 nm; applied voltage, 15 kV; BGE, 50 mM ammonium acetate, 30 mM OALS or SDS, pH 9.00.....67

Figure 3.8 Mass spectra of equimolar tryptophan and atenolol. Conditions: 500 μ L of tryptophan (25 mM in 0.5% formic acid) and 500 μ L of atenolol (25 mM in 0.5% formic acid). Conditions: negative mode; fragmentation energy, 80 V; solvent system, methanol. Tryptophan peak is $[M-H]^-$. Atenolol peak is $[M+FA-H]^-$ 69

Figure 3.9 Mass spectra of tryptophan and OALS at 0 minute and 7 minute. Mass spectra of SDS at 1 and 30 minute as control. Conditions: 475 μ L of tryptophan (25 mM in 0.5% formic acid) spiked with 25 μ L of OALS (25 mM in deionized water). Conditions: negative mode; fragmentation energy, 80 V; solvent system, methanol. Tryptophan peak is $[M-H]^-$ OALS peak is $[M]^-$ 70

Figure 3.10	<p>Ratio of OALS/tryptophan ESI-MS signal intensity over a period of 20 minutes in H₂O. Conditions: 475 μL of tryptophan (25 mM in 0.5% formic acid), pH 2.5, spiked with 25 μL of OALS (25 mM in deionized water). Conditions: fragmentation energy, 80 V; solvent system, methanol; Half-life of OALS, 48 s.....71</p>
Figure 3.11	<p>Tryptophan ESI-MS positive ion signal intensity (m/z = 205.0) over a period of 3 minutes in H₂O in a presence of OALS. Conditions: 475 μL of tryptophan (25 mM in 0.5% formic acid), pH 2.5, spiked with 25 μL of OALS (25 mM in deionized water). Conditions: fragmentation energy, 80 V; solvent system, methanol.....72</p>
Figure 3.12	<p>Ratio of OALS/tryptophan ESI-MS signal intensity over a period of 20 minutes in H₂O at 4 °C. Conditions: 475 μL of tryptophan (25 mM in 0.5% formic acid), pH 2.5, spiked with 25 μL of OALS (25 mM in deionized water). Conditions: fragmentation energy, 80 V; solvent system, methanol.....74</p>
Figure 3.13	<p>Ratio of OALS/atenolol ESI-MS signal intensity at 21°C and 60°C over a period of 20 minutes in H₂O showing an increase in the rate constant of OALS hydrolysis as temperature is increased. Conditions: 475 μL of tryptophan (5 mM ammonium acetate), pH 4.50, spiked with 25 μL of OALS (25 mM in deionized water). Conditions: fragmentation energy, 80 V; solvent system, methanol.....75</p>

Figure 3.14 Electropherogram of separation of phenol, resorcinol and 4-nitroaniline at 21 °C showing that OALS has not been hydrolyzed. Condition: detection, 214 nm; applied voltage, 15 kV; BGE, 5 mM ammonium acetate, 30 mM OALS, pH 4.50; capillary (50 µm ID) total length, 51.5 cm; effective length, 41.5 cm.....76

Figure 3.15 Electropherogram of separation of phenol, resorcinol and 4-nitroaniline at 60 °C showing that a good portion of OALS has been hydrolyzed. Condition: detection, 214 nm; applied voltage, 15 kV; BGE, 5 mM ammonium acetate, 30 mM OALS, pH 4.50; capillary (50 µm ID) total length, 51.5 cm; effective length, 41.5 cm.....78

LIST OF SYMBOLS AND ABBREVIATIONS

Symbol	Parameter
μ_{app}	apparent mobility
μ_{ep}	electrophoretic mobility
μ_{eof}	magnitude of electroosmotic flow
E	electric field
k'	retention factor
L_d	capillary length to the detector
L_t	total length of the capillary
N	theoretical plates
R_s	resolution
R^2	correlation coefficient
t_{eof}	migration time of EOF marker
t_m	migration time
t_{mc}	migration time of micelles
V	applied voltage (in volts)
UV	ultraviolet

ACN	acetonitrile
ALS	sodium 4-[(2-methyl-2-undecyl-1,3-dioxolan-4-yl) methoxy]-1-propane sulfonate
AU	absorbance unit
BGE	background electrolyte
CE	capillary electrophoresis
CIEF	capillary isoelectric focusing
CITP	capillary isotachopheresis
CMC	critical micelle concentration
CZE	capillary zone electrophoresis
DNA	deoxyribonucleic acid
EOF	electroosmotic flow
ESI-MS	electrospray ionization mass spectrometry
h	hour
HBA	hydrogen bond acceptor
HBD	hydrogen bond donor
HMUD	4-hydroxymethyl-2-methyl-2-undecyl-1,3-dioxolane
ID	inner diameter

IET	ion evaporation theory
LMT	sodium <i>N</i> -lauroyl- <i>N</i> -methyltaurate
LOD	limit of detection
MEKC	micellar electrokinetic chromatography
min	minute
NHB	non-hydrogen bonding
nm	nanometer
OALS	sodium 2,2-Bis(hexyloxy)propyl sulphate
PAGE	polyacrylamide gel electrophoresis
PF-MEKC	partial-filling micellar electrokinetic chromatography
RNA	ribonucleic acid
RSD	relative standard deviation
RBF	round-bottom flask
SDS	sodium dodecyl sulphate
SIDT	single ion in droplet theory
TOF ESI-MS	time-of-flight electrospray ionization mass spectrometry

CHAPTER 1 INTRODUCTION

1.1 CAPILLARY ELECTROPHORESIS

Electrophoresis is an analytical technique in which analytes are separated under the influence of an electric field. Arne Tiselius pioneered the use of electrophoresis as a separation technique in 1937 [1]. He separated albumin, alpha-, beta-, and gamma-globulins using moving boundary electrophoresis in this historical experiment. Tiselius went on to win the Nobel Prize in Chemistry in 1948 for his work in electrophoresis. Stellan Hjertén introduced capillary electrophoresis (CE) in 1967 using 3 mm tubes [2]. The separation of diverse analytes such inorganic ions, nucleotides and proteins using CE followed suit. However, the field remained stagnant till Jorgenson and Lukacs demonstrated high-efficiency separations (>400,000 theoretical plates) of fluorescent derivatives of amino acids, dipeptides and amines using 75- μm inner diameter (ID) open-tubular glass capillaries [3].

Performing electrophoresis in a narrow-bore capillary offers several advantages. The small ID capillary has a high surface-to-volume ratio compared to the slab gel traditionally used for electrophoresis. This allows for efficient dissipation of the heat generated by application of voltages as high as 30 kV [3]. Typically slab gel electrophoresis is limited to electric field (E) of 15 – 40 V/cm due to Joule heating. Up to 800 V/cm electric field can be applied to a capillary containing the same type of gel matrix [4]. The ability to perform electrophoresis separation at high voltage shortens the analysis time while simultaneously

enhancing the separation performance. The Furthermore, the small dimensions requires only minute amount of buffer or solvents, which means CE generates less toxic waste than alternative analytical technique such as high-performance liquid chromatography (HPLC).

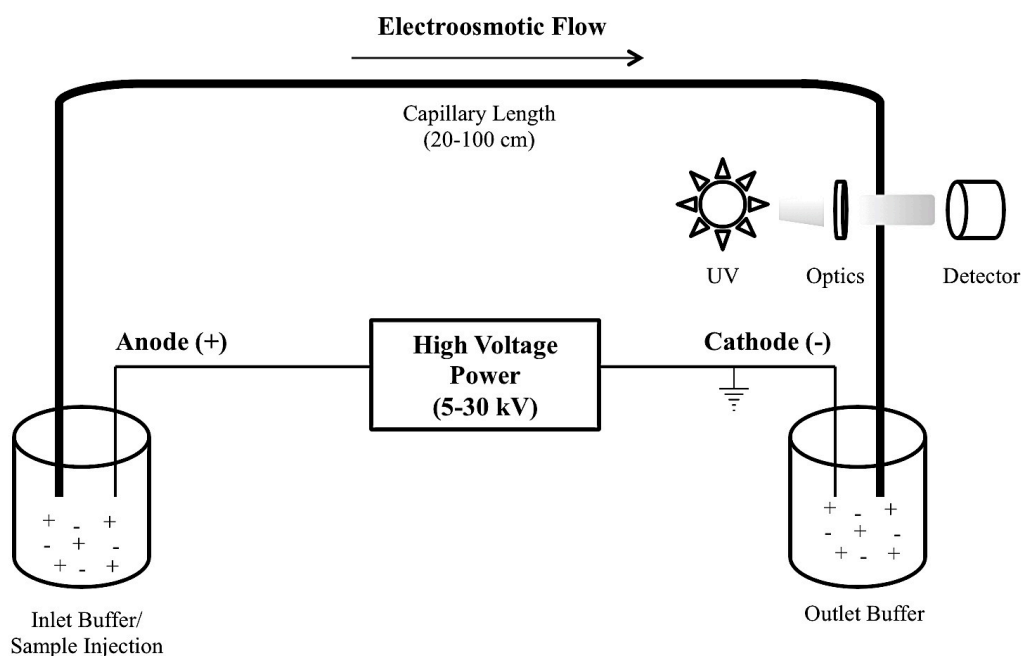


Figure 1.1 Schematic diagram of a CE instrument in normal polarity mode

CE can be performed under normal and reverse polarity. Figure 1.1 shows a schematic of a CE instrument in normal polarity mode. The instrument consists of a high voltage power supply (0-30 kV), a polyimide-coated capillary with an ID $\leq 100 \mu\text{m}$, two buffer containers (inlet and outlet) to accommodate the capillary and the electrodes connected to the power supply and a ultraviolet (UV) absorbance detector. In normal polarity, the cathode is in the outlet (detector) and the anode is in the inlet. In reverse polarity, the cathode is in the inlet and the anode is in the outlet (detector). When voltage is applied, two forces drive the

movement of the analytes. The first force is electrophoretic mobility (μ_{ep}). μ_{ep} is the direction and velocity of charged species. Under an applied voltage, analytes separate based on differences in their μ_{ep} . The analyte velocity is directly proportional to the magnitude of the voltage. Thus, electrophoretic separation at high voltage results in faster analysis time. Under normal polarity, if the applied field were the only force acting on the charged species, a cation would pass the detector, an anion would be moving away from the detector and a neutral analyte would be stationary. However, this is not the case. All analytes will actually pass the detector because in addition to μ_{ep} , there is a second force that moves the analytes. That force is called the electroosmotic flow (EOF).

EOF is the movement of liquid along a capillary upon the application of an electric field. It is the consequence of the ionized silanol groups on the interior capillary wall [5]. The EOF phenomenon is normally explained using the Stern-Gouy-Chapman model of the electrical double layer at a charged interface [6]. Silanol (SiOH) groups on the capillary wall are ionized to SiO⁻ under neutral or basic conditions. The SiO⁻ attracts cationic species from the buffer. This induces formation of a double layer also known as the Stern layer ≈ 0.1 nm. Application of an electric field across the length of the capillary causes the cations within the Stern layer to migrate towards the cathode along with their hydration spheres. The water molecules of the hydration spheres hydrogen-bond with water molecules of the bulk solution. This causes the entire buffer solution to be pulled towards the cathode [5]. Thus the net or apparent mobility (μ_{app}) of ions in capillary electrophoresis depends on both the electrophoretic mobility and the EOF (μ_{eof}):

$$\mu_{app} = \mu_{ep} + \mu_{eof} \quad (1-1)$$

The μ_{app} can be calculated from equation 1-2:

$$\mu_{app} = \frac{L_t L_d}{t_m V} \quad (1-2)$$

where L_t is the total length of the capillary (in cm), L_d is the distance from the inlet to the detector (in cm), t_m is the migration time of an analyte and V is the applied voltage (in volts). The μ_{eof} can be calculated using:

$$\mu_{eof} = \frac{L_t L_d}{t_{eof} V} \quad (1-3)$$

where t_{eof} is the migration time of an EOF marker (methanol).

As mentioned above, the migration of the analyte in CE is caused by μ_{ep} of the substance and the EOF. EOF affects the separation in CE. Hence, it is of a great interest to control the EOF. The most common factors used to control the EOF are: the pH and ionic strength of the buffer; addition of organic modifier and coating the inner capillary wall [7-11]. Changing the pH and ionic strength of the buffer is the easiest thing to do to control the EOF. Lowering the pH and

increasing the ionic strength of the buffer decrease the EOF. Smaller fraction of the silanol groups is deprotonated at lower pH resulting in thinner Stern layer. The higher ionic strength also compresses the Stern layer. Compression of the Stern layer results in a lower zeta potential and hence, lower EOF [7, 9].

There are a few modes of CE. The most common and basic mode of CE is the capillary zone electrophoresis (CZE). CZE cannot separate neutral analytes. In CE, analytes separate according to their individual μ_{ep} . What happens when the analytes are not charged? Uncharged analytes would not have μ_{ep} . They would be driven to the detector solely by the EOF. Therefore, there would not be any separation. Other modes of CE include capillary isotachopheresis (CITP) [12, 13], capillary isoelectric focusing (CIEF) [14] and micellar electrokinetic chromatography (MEKC) [15, 16]. With respect to the separation of neutral analytes, MEKC is the most interesting mode of CE.

1.2 MICELLAR ELECTROKINETIC CHROMATOGRAPHY

1.2.1 Principle of Micellar Electrokinetic Chromatography

Micellar electrokinetic chromatography (MEKC) was introduced by Shigeru Terabe in 1984 [17]. MEKC is a high-efficiency separation technique, capable of easily achieving greater than 100,000 theoretical plates (N). If N is lower than 100,000, the MEKC condition is not optimum [16]. MEKC has become a popular separation technique with analytes ranging from small molecules to large molecules such as peptides, proteins, lipids and saccharides [17-22]. The number of publications for the routine analysis using MEKC is

greater than the bibliography covering the method development of MEKC [23]. MEKC has presented itself as a viable alternative to the HPLC. For one, MEKC generates much less toxic waste.

Secondly, the pseudostationary phase can easily be changed if an analysis demands different selectivity to achieve satisfactory separation. There is no need to replace an expensive column. In MEKC, a chemical species called a *surfactant* is added to the buffer solution to create a pseudostationary phase. A surfactant is a chemical species that contain a hydrophobic tail and a hydrophilic head group. The hydrophobic tail component can be single-tailed as shown in Figure 1.2 or double-tailed [24]. In MEKC, the head group must be ionic to act as a pseudostationary phase. Thus for the purpose of this thesis, only single-tailed ionic surfactants are discussed.

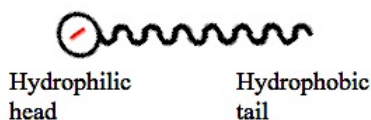


Figure 1.2 Structure of surfactant

When surfactants are dissolved in aqueous solvent (i.e. water), the hydrophobic group distorts the structure of water. This distortion increases the free energy of the system. The aqueous system responds by minimizing contact between the hydrophobic tail and the surrounding water [24]. There are two ways the system achieves this. First, the surfactant molecules are expelled to the interface between the liquid (water) and gas phase (air). The surface of the water is covered with a single layer of surfactant with the hydrophobic tail oriented predominantly toward

the air and the hydrophilic head anchored in the liquid phase. Air is non-polar in nature and decreases the dissimilarity of the two phases contacting each other in the surface. However, as the surfactant concentration increases, the increase in the free energy of the system can no longer be countered by expelling surfactant molecules to the surface of the water.

Micellization is an alternative mechanism to reduce the free energy of the system by minimizing the contact between the hydrophobic tail and water [24]. The concentration at which surfactant starts forming micelles is called the *critical micelle concentration* (CMC). Above its CMC, extra surfactant added to the solution forms ionic micelles consisting of a hydrophobic core, hence minimizing the contact between the hydrophobic tail and water. The surfactant monomer and its ionic micelles are in equilibrium above the CMC (Fig. 1.3).

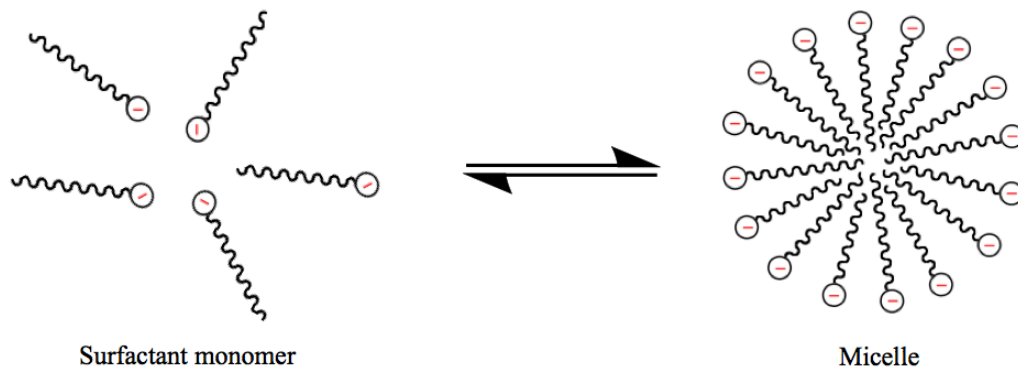


Figure 1.3 Equilibrium between surfactant monomer and its micelle above the CMC.

The ionic micelle has an μ_{ep} and acts as a pseudostationary phase in MEKC. The neutral analytes will partition into the hydrophobic core of ionic micelles, and consequently gain an apparent μ_{ep} . Different analytes would have

different distribution equilibrium with the micelle. Some analytes would be more incorporated into the micelle while others may not. The more the analyte is incorporated, the higher the apparent mobility. The analyte is also driven by the EOF. Therefore, the migration time of the analyte in MEKC is a function of the distribution coefficient, the μ_{ep} of the micelle, and the EOF [16, 25, 26]. Figure 1.4 illustrates the principle of MEKC. Most commonly, the EOF is stronger than the μ_{ep} of the anionic micelle. The anionic micelle migrates towards the anode dragging analytes incorporated into the micelle along with it. However, the EOF is stronger than the μ_{ep} of the micelle. Thus, the net movement of the micelle is towards the cathode. Unlike HPLC, the micelles are not truly stationary and so are referred to as a *pseudostationary phase*, i.e., a phase that moves slower than the aqueous buffer.

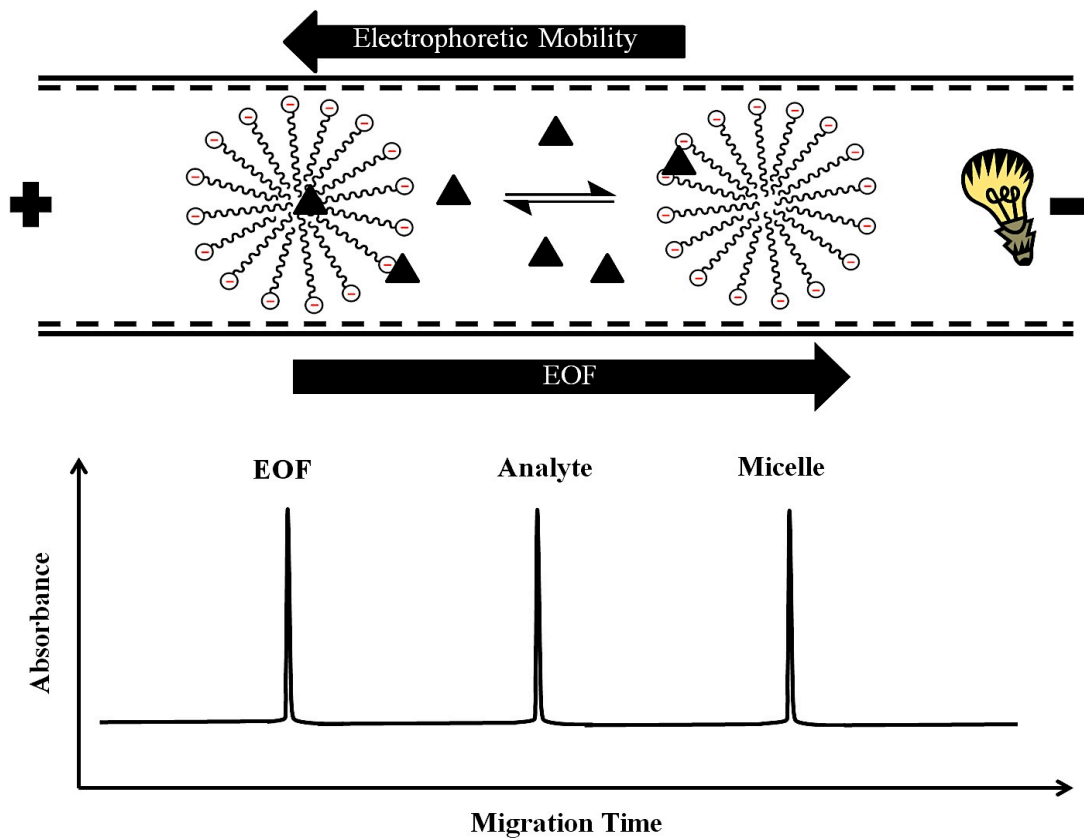


Figure 1.4 Schematic illustration of the principle of MEKC with anionic micelle and stronger EOF under normal polarity

The analyte moves at a velocity between that of the EOF and the micelle. This means the migration time of a neutral analyte (t_m) falls in between the migration time of the EOF (t_{eof}) and the migration time of the micelle (t_{mc}). The ratio of the t_{mc} and t_{eof} is known as the migration time window [27]. A faster micelle mobility results in larger t_{mc} and hence broader migration time window.

The separation in MEKC is based on the equilibrium of a neutral analyte between the aqueous buffer and the hydrophobic micelle. Simply flushing the capillary and adding a different surfactant to the buffer will create a different pseudostationary phase with a different selectivity [16].

1.2.2 Selectivity of the Pseudostationary Phase

The resolution (R_s) of an MEKC separation is given by equation 1-4 [26, 28]. R_s is affected by the separation efficiency (N), the retention factor (k'), the size of the migration time window (t_{mc}/t_{eof}) and α is the selectivity factor (k_2'/k_1') where k_1' and k_2' are the retention factor of analytes 1 and 2 respectively.

$$R_s = \frac{\sqrt{N}}{4} \left(\frac{\alpha - 1}{\alpha} \right) \left(\frac{k_2'}{1 + k_2'} \right) \left(\frac{1 - \frac{t_{eof}}{t_{mc}}}{1 + \left(\frac{t_{eof}}{t_{mc}} \right) k_1'} \right) \quad (1-4)$$

The selectivity factor is the most important and effective parameter to optimize the R_s . The selectivity factor quantifies the relative difference in distribution equilibrium between analytes 1 and 2 with the micelle. Distribution equilibrium is a unique characteristic for a given micellar and aqueous system. Therefore, changing the surfactant will modify the distribution equilibrium and consequently different selectivity factor. Based on the selectivity factor, an appropriate pseudostationary phase can be chosen to achieve the optimum separation [26, 29, 30]. The main type of interaction between the micelle and the analyte is hydrophobic interaction [25]. The more hydrophobic an analyte, the deeper it is integrated into the hydrophobic core of the micelle. Hydrophobic analyte spends on average more time inside the micelle than in the aqueous bulk solution compared to hydrophilic analyte. Highly hydrophobic analyte would have a t_m closer to t_{mc} .

A parameter to probe the interaction between micelle and analyte is the retention factor (k'). k' of a neutral analyte with a pseudostationary phase can be calculated using [26]:

$$k' = \frac{t_m - t_{eof}}{t_{eof} \left[1 - \left(\frac{t_m}{t_{mc}} \right) \right]} \quad (1-5)$$

where t_m is the migration time of the analyte, t_{eof} is the migration time of the EOF (usually measured by injecting methanol) [31] and t_{mc} is the migration time of the micelle (mobility of the pseudostationary phase). Higher k' indicates greater incorporation of the analyte inside the micelle. Calculating k' for a group of analytes at a given pseudostationary phase provides information about the selectivity of the pseudostationary phase. However, the mobility of the pseudostationary phase needs to be determined before k' can be calculated.

1.2.3 Mobility of the Pseudostationary Phase

The mobility of the pseudostationary phase is needed to calculate the k' and determine the selectivity factor of the pseudostationary phase. The mobility of the pseudostationary phase is also used to determine the migration time window. For instance, a faster micelle mobility results in greater migration time window, and hence larger peak capacity. Peak capacity is the maximum number of peaks that can fit into the migration time window and where each peak is separated from adjacent peaks with $R_s = 1$ [32]. Two ways to determine the mobility of the

pseudostationary phase are the single-marker method and the homologous series method [33, 34].

1.2.3.1 Single-marker Method

In the single-marker method, a highly hydrophobic solute (micelle marker) is added to the sample solution. The main type of interaction in MEKC between pseudostationary phase and the solute is hydrophobic interaction. The micelle marker would partition deep inside the micelle. The micelle marker would spend all its time in the core of the micelle and negligible time in the bulk solution. The micelle marker would technically have the same mobility as the micelle which means $t_m = t_{mc}$. Some examples of micelle markers are Sudan III, dodecanophenone and anthracene [17, 35, 36]. However, a compound that is fully immersed in the core of the pseudostationary phase does not exist. A micelle marker would spend a little amount of time outside of the micelle. Thus, the t_{mc} given by a single-marker method is not the “true” migration time of the pseudostationary phase. Rather, it is a good approximation of the t_{mc} .

The single-marker method gets even more problematic when organic solvents are added to the buffer. Addition of organic solvents helps to solubilize hydrophobic analytes and it also decreases the t_{eof} . Decreasing the t_{eof} increases the migration time window of the MEKC separation. However, the addition of the organic solvents also means that the micelle marker spends more time in the bulk solution. The micelle marker is not fully incorporated into the micelle which means t_m is no longer equal to t_{mc} [37].

1.2.3.2 Homologous Series Method

As discussed in Section 1.2.3.1, there are some limitations in using a single-marker to determine the mobility of the pseudostationary phase. An alternative way to calculate the mobility of the pseudostationary phase is using a homologous series method, as was introduced by Bushey and Jorgenson in 1989 [34]. The homologous series is a series of compounds that differ by one methyl group. Figure 1.5 shows the homologous series of alkylphenones (acetophenone – hexanophenone).

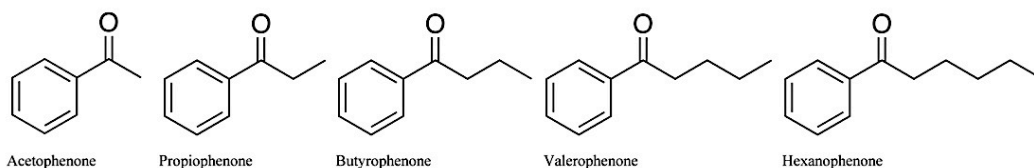


Figure 1.5 Alkylphenone homologous series (acetophenone – hexanophenone)

In this method, the alkylphenones are separated under MEKC conditions. Next, the t_m of the alkylphenone with the highest carbon number is assigned as the t_{mc} . The k' of each alkylphenone is then calculated according to equation 1-5. The $\log k'$ is plotted against the carbon number. Ideally the plot should be linear. If it is not, new $\log k'$ are calculated by extrapolating the regression line to the member of the homologous series with the highest carbon number. The new $\log k'$ is used to calculate the new t_{mc} by rearranging equation (1-5):

$$t_{mc} = \frac{t_m}{1 - \frac{t_m - t_{eof}}{k' t_{eof}}} \quad (1-6)$$

The new t_{mc} is used to recalculate the $\log k'$ of each homologous series compound and again plotted against the carbon number. The reiteration is repeated until the difference between consecutive t_{mc} values is less than 0.001 min or the correlation coefficient reaches $R^2 = 0.9999$. The number of iteration needed depends on the member of the homologous series with the highest carbon number. The higher the carbon number the iteration is started with, the closer the t_m is to the actual t_{mc} and fewer iterations are needed. Typically, 50-100 iterations are needed [33]. The t_{mc} is used to calculate the apparent mobility of the micelle (μ_{app}) using equation 1-2. The mobility of the micelle (μ_{ep}) can be calculated from equation 1-1 using μ_{app} and μ_{eof} .

Alkylphenones (Fig. 1.5) are the homologous series used to determine t_{mc} in this thesis. Other homologous series that have been used are dansylated alkylamines and alkylbenzenes [34, 38]. The homologous series method has been used extensively to measure the mobility of pseudostationary phase since its inception [33]. However, it is not infallible. There are some cases where it has failed to determine the mobility of a pseudostationary phase [39-41]. In those cases, the plot of $\log k'$ vs. carbon number is not linear and the iterative calculations do not converge. The $\log k'$ vs. carbon number plot either displays negative [39] or positive deviation [41]. Figure 1.6 displays the positive deviation of the $\log k'$ vs. carbon number plot for an acid-labile surfactant (Chapter 2 and ref. [41]). Despite a few shortcomings, the homologous-series method is more accurate in determining the micelle mobility compared to the single marker method.

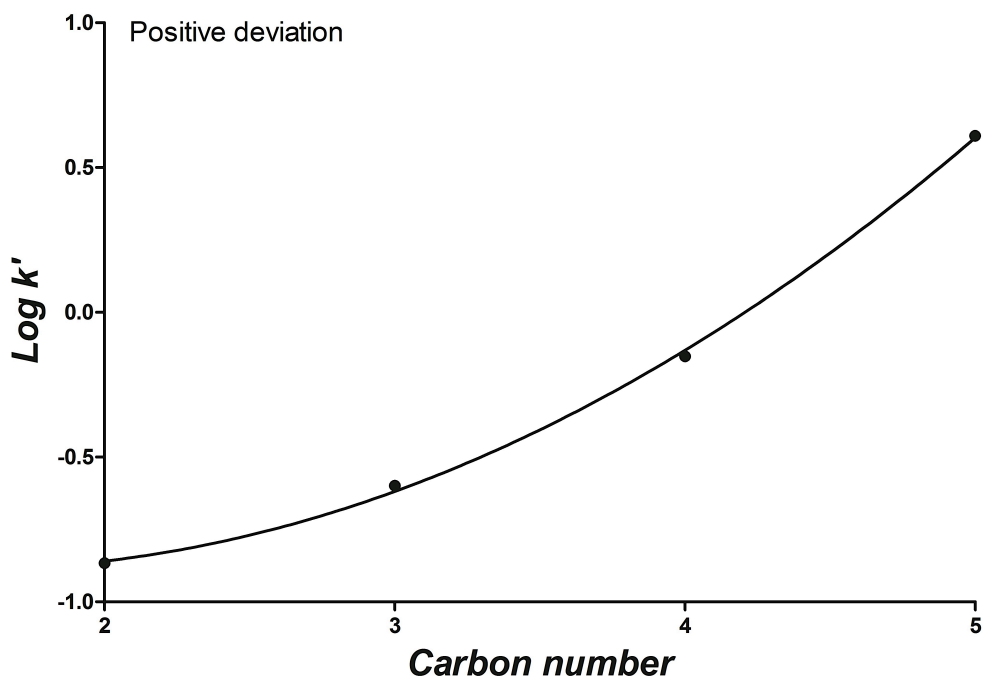


Figure 1.6 Positive deviation of plot of $\log k'$ vs. carbon number of alkylphenones. The pseudostationary phase is an acid-labile surfactant [41].

1.3 ELECTROSPRAY IONIZATION MASS SPECTROMETRY

1.3.1 Brief history of electrospray ionization mass spectrometry

Electrospray ionization was pioneered by Malcolm Dole in 1968 [42]. Yamashita and Fenn revisited Dole's work in 1984 and coupled electrospray ionization with a mass spectrometer [43]. Since then, electrospray ionization mass spectrometry (ESI-MS) has become an invaluable analytical technique for the analysis of large and small molecules. ESI-MS has been used extensively to study small molecules in the pharmaceutical industry drug development process [44-46]. ESI-MS is an essential tool in many of the important drug discovery processes such as determination of the purity of the compound, pharmacokinetics and toxicology [44]. The ESI-MS is also used to study the interaction of small

molecules with variety of biomolecule targets such as nucleic acids, proteins, RNA and DNA [46-48]. ESI-MS is heavily used in the field of metabolomics. Metabolomics is a qualitative and quantitative study of low-molecular-weight compounds that participate in the general metabolic reactions in the biological samples [49, 50]. It is an indispensable tool in metabolomics and the chemistry Nobel Prize awarded in 2002 to J.B. Fenn recognizes the importance and impact of ESI-MS in the chemistry field.

ESI-MS is also a very popular analytical technique to study large biomolecules such as proteins. The field of proteomics that deals with the study of proteins (primary sequence, post-translational modifications or protein-protein interactions) has made use of ESI-MS extensively [51].

1.3.2 Ion Formation Mechanism

There are four major processes leading to the generation of charged analyte in ESI [52]. Analytes must be charged when they reach the detector to appear in an ESI spectrum. The four major processes are the production of charged droplets at the ESI capillary tip, the shrinkage of charged droplets by evaporation with dry nitrogen gas, repeated Coulombic explosions and finally the generation of gas phase ions. The schematic of an ESI instrument illustrating the four processes is shown in Figure 1.7.

In ESI-MS, a high voltage (2000 – 4000 V) is applied to a metal capillary where liquid passes through. In the positive ionization mode, a positive potential is applied to the capillary. Positive ions in the liquid accumulate at the liquid

surface. The accumulation of positive charges on the surface of the liquid causes a Taylor cone to form as the liquid exits the capillary [53]. When the charges build-up reaches sufficiently high electric field, the Taylor cone becomes unstable and a liquid filament is formed. The liquid filament surface contains a high concentration of positive ions. At a distance away (1-3 cm) [54] from the capillary tip (downstream), the liquid filament destabilizes and breaks into positively charged droplets (Fig 1.7).

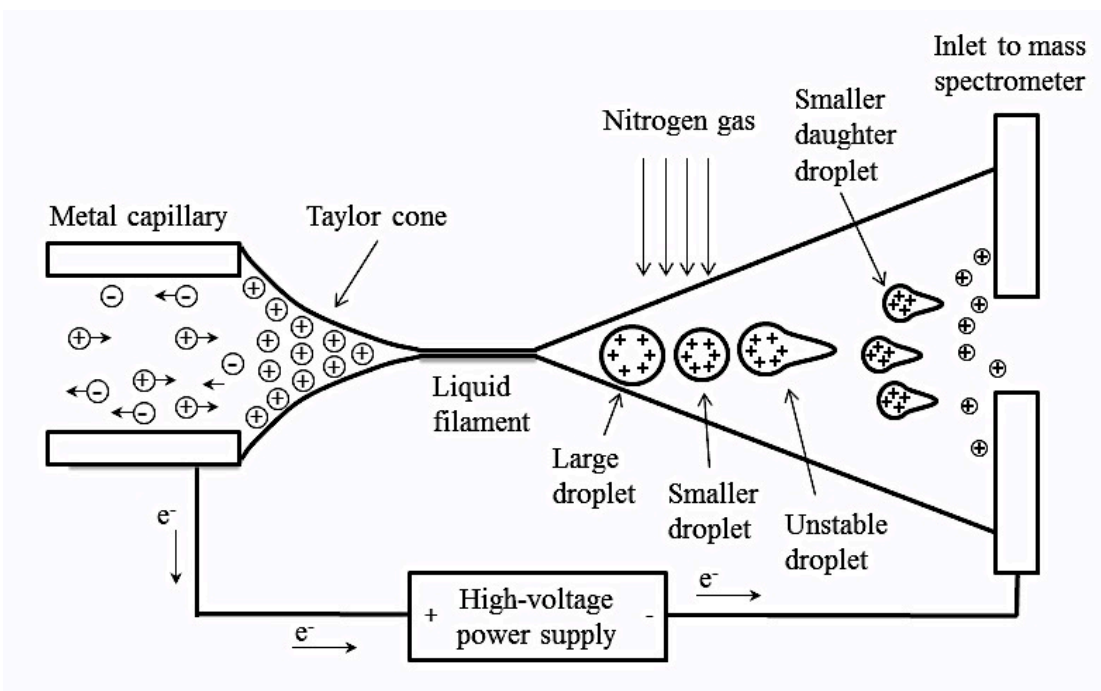


Figure 1.7 Schematic of ion formation in ESI-MS

Once a charged droplet is formed, it is going to continue to migrate towards the inlet of the mass spectrometer due to its negative applied potential. The next major process is the shrinkage of the charged droplets. Dry nitrogen gas flowing across the charged droplets evaporates the solvents from the droplets.

This process reduces the volume of the droplets, hence increasing the charge concentration within an individual droplet.

The third process is the repeated disintegration of the charged droplet. As the droplets get smaller, the charge concentration increases. Concurrently the Coulombic repulsion of the ions within the droplet increases, until it overcomes the surface tension of the solvent [55]. This condition is known as the Rayleigh limit. Once the droplets have shrunk to the Rayleigh limit, repeated Coulombic explosions occur [56]. This process is followed by the generation of gas phase ion.

There are two proposed mechanisms for the generation of gas phase ions in ESI-MS. They are the Single Ion in Droplet Theory (SIDT) [42] and the Ion Evaporation Theory (IET) [57]. In the SIDT, Dole and co-workers theorized that the repeated Coulombic explosions resulted in the formation of extremely small droplets (radius ≈ 1 nm) containing a single ion. The subsequent evaporation of the solvent around the droplet resulted in the formation of the gas phase ion.

Iribarne and Thompson developed the IET from transition state theory. They proposed that an ion could be ejected from the droplet before the Rayleigh limit of the droplet was reached and the Coulombic explosions occurred. The hypothesis is that as the droplets become smaller and approach the Rayleigh limit, some ions must be expelled from the droplet because the electric field at liquid surface becomes too high. The ion evaporates from the droplet into the gas phase to relieve the repulsion of ions inside the droplet. In conclusion, there is no clear evidence to support solely one mechanism over the other. The IET theory is well-

supported for small ions, but the SIDT theory is more plausible to apply to very large ions [54].

1.3.3 Ion Suppression in ESI-MS by Surfactant

The analyte in a solution would ideally become a charged gas phase species when it is electrosprayed and analyzed by the mass spectrometer. However, there are other pathways that the analyte can take [58]. The analyte may precipitate out of the solution. The analyte could remain as a neutral species and be deposited in the interface of the mass spectrometer. Alternatively, the analyte can be turned into a gas phase ion and get detected by the instrument. Things that decrease the production rate of small droplets reduce the amount of gas phase ions. The reduction in the amount of gas phase ions leads to diminished signal i.e. ion suppression [56, 59].

Surfactants such as sodium dodecyl sulphate (SDS) are well known to cause ion suppression in ESI-MS [60, 61]. SDS suppresses the ESI-MS signal even at concentrations below the CMC. This shows that the surfactant is incompatible with ESI-MS even at low concentration. Rundlett and Armstrong explained the suppression effect caused by SDS using a modified aerosol ionic redistribution (AIR) model [61].

The surfactant has a hydrophobic tail and a hydrophilic head. The hydrophobic tail distorts the structure of the solvent in the droplet and increases the free energy of the system. The system responds by minimizing contact between the hydrophobic tail and the solvent [24]. The system accomplishes this

by expelling the surfactant to the surface of the droplet with the hydrophobic tail oriented towards the gas phase and the hydrophilic head anchored in the interior of the droplet as shown in Figure 1.8. Thus the surfactants are concentrated at the surface of the droplet. The third major process of ion formation in ESI-MS is repeated disintegration of the charged droplets when the Rayleigh limit is reached. The repeated disintegration of the charged droplets produce smaller daughter droplets. The daughter droplets contain the species that resides on the surface of the parent droplets [52, 56]. Since the daughter droplet is smaller, the concentration of surfactant on the surface gets even greater. High concentration of surfactant at the surface of the droplets impedes the ability of the analyte to get to droplet surface, and thus to the gas phase. This results in the ion suppression.

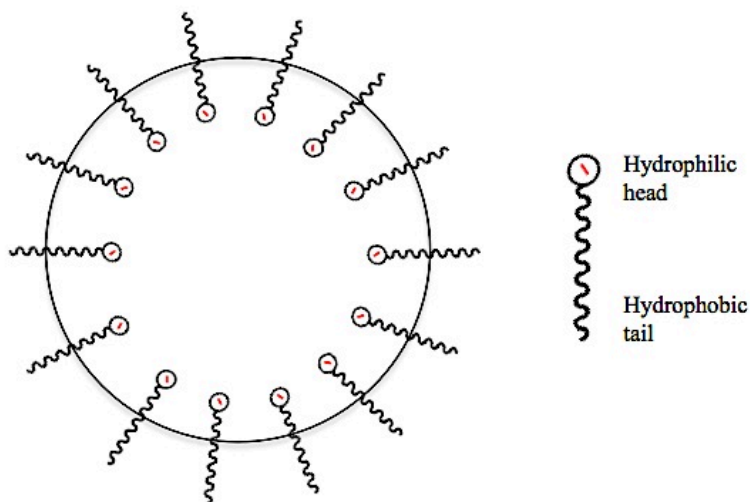


Figure 1.8 Surfactant monomers at the liquid-air interface inside a droplet [61]. The hydrophobic tail is oriented towards the gas phase while the hydrophilic head is anchored in the inner of the droplet.

Some techniques have been developed to couple MEKC with ESI-MS [62, 63]. One method is partial-filling MEKC (PF-MEKC) [29, 64]. In PF-MEKC, a plug of BGE, micellar solution and sample solution is present respectively in the

capillary. Upon the application of voltage, the analytes migrate into the micellar region and are separated. The separated analytes continue to move towards the BGE region free of surfactant and are introduced into the ESI-MS. Meanwhile, the micellar region stays inside the capillary hence avoiding the ion-suppression. Another method is using volatile surfactants such as perfluorooctanoic acid (PFOA). PFOA is volatile and does not accumulate at the surface of the droplets to suppress the analyte signal [65, 66]. As briefly discussed in Section 1.3.3, polymeric surfactants have also been used to couple MEKC with ESI-MS [67-69]. Polymeric surfactants are synthesized from surfactants containing a polymerizable group in the hydrophobic tail. The surfactants are polymerized well above the CMC to form polymeric micelles. In polymeric micelles, the surfactant monomers are held together by covalent bonds [69]. Some examples of polymeric micelles are sodium poly(N-undecanoyl-L-glycinate) and sodium poly(N-undecanoyl-L-leucylvalinate) and butyl acrylate-butyl methacrylate-methacrylic acid copolymer sodium salt [70, 71]. Polymeric micelles do not suppress the analyte ion signals in ESI-MS. The reason proposed is the high volatility of the polymer micelle [71]. However, the polymeric micelle is not as surface active as the smaller surfactant [61]. The concentration of the polymeric micelle at the surface of the droplet is much lower. This makes it easier for analyte ion to get to the gas phase and detected by the mass spectrometer. The lack of surface-activity of polymeric micelles further supports that low-molecular weight surfactants prevent the analyte ion to get to the surface of the droplet resulting in the suppression of the

analyte ion. Lastly, surfactant containing ketal-linkage can be acid-hydrolyzed into ESI-MS compatible degradation products [41].

1.4 CLEAVABLE SURFACTANTS

1.4.1 Acid-labile Surfactant

Cleavable surfactants are stable under neutral aqueous conditions, but can be degraded when the conditions are changed. Some of the ways cleavable surfactants are cleaved are UV irradiation, alkaline hydrolysis and acid hydrolysis [72-75]. Surfactants that has an azo group between the hydrophobic tail and the ionic head are sensitive to UV irradiation [76]. An example of an alkaline-labile surfactant is quaternary ammonium compounds containing an ester bond. Jaeger and co-workers synthesized the first cleavable surfactant that contains a cyclic ketal functional group in the palisade region and can be hydrolyzed under acidic condition [77]. This thesis focuses on ketal based acid labile surfactants.

Synthetic chemists use ketal functionalities extensively to protect carbonyl groups from nucleophilic attack. Ketal is a molecule derived from a ketone. Ketal contains two single-bonded oxygen atoms attached to the same carbon atom (see Fig 1.9). Ketal protection is very popular because it is a reversible process. Ketals can be easily acid-hydrolyzed back to its corresponding ketone [78]. Figure 1.9 shows a general reaction scheme of an acid-hydrolysis of a ketal. This reversibility prompted the use of ketals as a linkage between the hydrophobic tail and the hydrophilic head of a surfactant [77, 79].

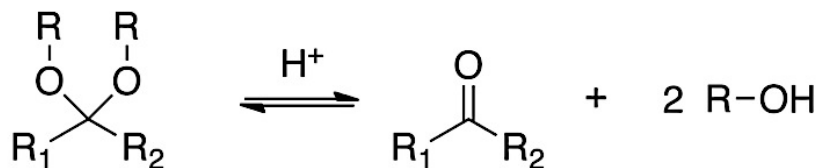


Figure 1.9 Equilibrium between a ketal and its corresponding ketone

1.4.2 Surfactants with an Acid-labile Ketal-linkage

The introduction of the ESI-MS has facilitated the growth of the field of proteomics (Section 1.3.1). Surfactants are heavily used in proteomics to solubilize, stabilize and denature proteins, especially hydrophobic membrane proteins [60]. However, as discussed in Section 1.3.3 surfactants cause ion suppression and interfere with subsequent analysis in the ESI-MS [58, 60, 61]. All surfactant must be removed from the mixture of proteins and surfactant prior to the ESI-MS analysis. This is where acid-labile surfactants come into play. The acid-labile surfactant can be used to treat the proteins and hydrolyzed before the analysis with the ESI-MS. Acid-labile surfactant hydrolyzes readily at pH 4-5 at the room temperature [74, 75]. The hydrolysis products of acid-labile surfactant do not suppress the analyte signal in ESI-MS. Therefore, the mixture of proteins and hydrolyzed acid-labile surfactant can be readily injected into ESI-MS for analysis. There is no need to remove the hydrolyzed acid-labile surfactant prior to analysis. This is making it an attractive alternative to traditional non-degradable surfactant used in proteomics such as SDS.

An example of an acid-labile surfactant that is used heavily in proteomics is sodium 4-[(2-methyl-2-undecyl-1,3-dioxolan-4-yl) methoxy]-1-propane

sulfonate (ALS, Figure 1.10) [80, 81]. ALS contains a cyclic ketal linkage in the palisade region that makes it acid-hydrolyzable. ALS is commercially distributed by Waters under the trade name RapiGest™. It was introduced in 1999 to replace SDS in polyacrylamide gel electrophoresis (PAGE) because it has a similar denaturing and electrophoretic properties as SDS [80]. ALS has also been used to separate proteins in a microfluidic devices [41, 82].

Another ketal-linkage containing surfactant which was recently introduced is sodium 2,2-Bis(hexyloxy)propyl sulphate (OALS, Figure 1.10) [83]. OALS contains an acyclic ketal linkage. Acyclic ketal linkage is more labile compared to its cyclic counterpart [78, 84]. Figure 1.10 shows the structure of ALS and OALS.

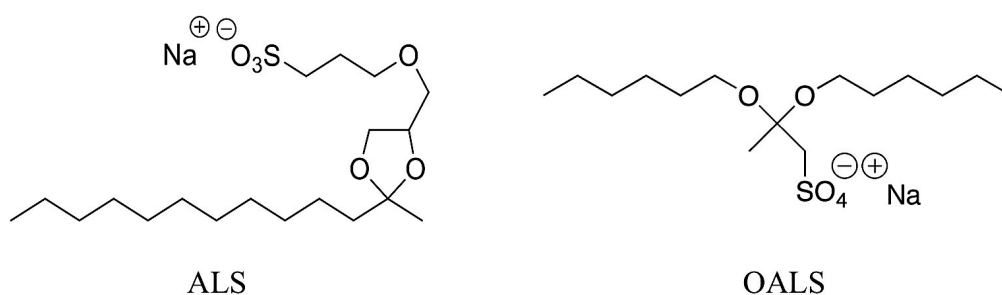


Figure 1.10 Structures of ALS (cyclic ketal) and OALS (acyclic ketal)

1.5 OUTLINE OF THESIS

MEKC is a powerful separation technique that can give separation efficiency exceeding 100,000 theoretical plates. ESI-MS is a powerful detection technique that gives rich structural information. The combination of MEKC with the ESI-MS is very tempting. However, the presence of surface-active surfactant

in the MEKC that suppresses analyte signal in ESI-MS makes the hyphenation between these two techniques difficult.

This thesis studies two types of acid-labile surfactants and their compatibility with ESI-MS. Acid-labile surfactant has been used to separate proteins in microfluidic electrophoresis devices [82], but this is the first time that acid-labile surfactants are used in MEKC of small molecules prior to ESI-MS. This is also the first evaluation of acid-labile surfactants for MEKC-ESI-MS in both offline and online modes. In Chapter 2, the potential of ALS as a pseudostationary phase in MEKC is assessed. Also, the kinetics and hydrolysis rate of ALS are determined. Lastly, the compatibility of hydrolysis products of ALS with ESI-MS is investigated. In Chapter 3, the potential to use OALS in an MEKC separation is tested. The kinetics of OALS is also determined along with the compatibility of the degradation products with ESI-MS. The use of temperature to control the hydrolysis rate of OALS is also shown. Finally, Chapter 4 summarizes the key discoveries within this thesis and suggests some further areas for investigation.

1.6 REFERENCES

- [1] A. Tiselius, *T. Faraday. Soc.*, 33 (1937) 524.
- [2] S. Hjertén, *Chromatogr. Rev.*, 9 (1967) 122.
- [3] J.W. Jorgenson, K.D. Lukacs, *Anal. Chem.*, 53 (1981) 1298.
- [4] M.J. Rocheleau, N.J. Dovichi, *J. Microcolumn. Sep.*, 4 (1992) 449.
- [5] T.S. Stevens, H.J. Cortes, *Anal. Chem.*, 55 (1983) 1365.
- [6] F.F. Cantwell, S. Puon, *Anal. Chem.*, 51 (1979) 623.
- [7] B.B. VanOrman, G.G. Liversidge, G.L. McIntire, T.M. Olefirowicz, A.G. Ewing, *J. Microcolumn. Sep.*, 2 (1990) 176.
- [8] C. Schwer, E. Kenndler, *Anal. Chem.*, 63 (1991) 1801.
- [9] M.A. Hayes, I. Kheterpal, A.G. Ewing, *Anal. Chem.*, 65 (1993) 27.
- [10] C.A. Lucy, R.S. Underhill, *Anal. Chem.*, 68 (1996) 300.
- [11] S. Terabe, H. Utsumi, K. Otsuka, T. Ando, T. Inomata, S. Kuze, Y. Hanaoka, *J. High. Resolut. Chromatogr.*, 9 (1986) 666.
- [12] D. Kaniansky, J. Marák, *J. Chromatogr. A*, 498 (1990) 191.
- [13] P. Blatny, F. Kvasnicka, *J. Chromatogr. A*, 834 (1999) 419.
- [14] R. Rodriguez-Diaz, T. Wehr, M. Zhu, *Electrophoresis*, 18 (1997) 2134.
- [15] S. Terabe, K. Otsuka, T. Ando, *Anal. Chem.*, 57 (1985) 834.
- [16] S. Terabe, *Annu. Rev. Anal. Chem.*, 2 (2009) 99.
- [17] S. Terabe, K. Otsuka, K. Ichikawa, A. Tsuchiya, T. Ando, *Anal. Chem.*, 56 (1984) 111.
- [18] B. Stanley, K.A. Mehr, T. Kellock, J.D. Van Hamme, K.K. Donkor, *J. Sep. Sci.*, 32 (2009) 2993.

- [19] P.J. Oefner, C. Chiesa, *Glycobiology*, 4 (1994) 397.
- [20] J.M. Sanchez, V. Salvado, *J. Chromatogr. A*, 950 (2002) 241.
- [21] H. Shadpour, S.A. Soper, *Anal. Chem.*, 78 (2006) 3519.
- [22] F.A. Tomas-Barberan, *Phytochem. Anal.*, 6 (1995) 177.
- [23] M. Silva, *Electrophoresis*, 30 (2009) 50.
- [24] M.J. Rosen, *Surfactants and Interfacial Phenomena*, John Wiley & Sons, Inc., Hoboken, New Jersey, 3rd ed., 2004.
- [25] S. Terabe, *Anal. Chem.*, 76 (2004) 240A.
- [26] S. Terabe, *Chem. Rec.*, 8 (2008) 291.
- [27] C.-X. Zhang, Z.-P. Sun, D.-K. Ling, *J. Chromatogr. A*, 655 (1993) 309.
- [28] J.G. Bumgarner, M.G. Khaledi, *Electrophoresis*, 15 (1994) 1260.
- [29] M. Silva, *Electrophoresis*, 32 (2011) 149.
- [30] S. Yang, M.G. Khaledi, *Anal. Chem.*, 67 (1995) 499.
- [31] E. Fuguet, C. Ràfols, E. Bosch, M. Rosés, *Electrophoresis*, 23 (2002) 56.
- [32] L.R. Snyder, J.J. Kirkland, J.W. Dolan, in: *Introduction to Modern Liquid Chromatography*, John Wiley & Sons, Inc., Hoboken, New Jersey, 2010.
- [33] S.K. Wiedmer, J. Lokajova, M.L. Riekkola, *J. Sep. Sci.*, 33 (2010) 394.
- [34] M.M. Bushey, J.W. Jorgenson, *Anal. Chem.*, 61 (1989) 491.
- [35] P. Morin, J.C. Archambault, P. Andre, M. Dreux, E. Gaydou, *J. Chromatogr. A*, 791 (1997) 289.
- [36] W.E. Wall, D.J. Allen, K.D. Denson, G.I. Love, J.T. Smith, *Electrophoresis*, 20 (1999) 2390.
- [37] N. Chen, S. Terabe, T. Nakagawa, *Electrophoresis*, 16 (1995) 1457.

- [38] P.G.H.M. Muijselaar, H.A. Claessens, C.A. Cramers, *Anal. Chem.*, 66 (1994) 635.
- [39] D.S. Peterson, C.P. Palmer, *Electrophoresis*, 22 (2001) 1314.
- [40] C.P. Palmer, N. Tanaka, *J. Chromatogr. A*, 792 (1997) 105.
- [41] B. Stanley, C.A. Lucy, *J. Chromatogr. A*, 1226 (2012) 55.
- [42] M. Dole, L.L. Mack, R.L. Hines, R.C. Mobley, L.D. Ferguson, M.B. Alice, *J. Chem. Phys.*, 49 (1968) 2240.
- [43] M. Yamashita, J.B. Fenn, *J. Phys. Chem.*, 88 (1984) 4451.
- [44] S.A. Hofstadler, K.A. Sannes-Lowery, *Nat. Rev. Drug Discovery*, 5 (2006) 585.
- [45] J. Zhang, G. McCombie, C. Guenat, R. Knochenmuss, *Drug Discovery Today*, 10 (2005) 635.
- [46] S.A. Hofstadler, R.H. Griffey, *Chem. Rev.*, 101 (2001) 377.
- [47] B. Ganem, Y.T. Li, J.D. Henion, *J. Am. Chem. Soc.*, 113 (1991) 6294.
- [48] F. Rosu, E. De Pauw, V. Gabelica, *Biochimie*, 90 (2008) 1074.
- [49] W.B. Dunn, D.I. Ellis, *TrAC, Trends Anal. Chem.*, 24 (2005) 285.
- [50] R. Ramautar, G.W. Somsen, G.J. de Jong, *Electrophoresis*, 30 (2009) 276.
- [51] R. Aebersold, M. Mann, *Nature*, 422 (2003) 198.
- [52] P. Kebarle, L. Tang, *Anal. Chem.*, 65 (1993) 972A.
- [53] G. Taylor, *Proc. R. Soc. London, Ser. A*, 280 (1964) 383.
- [54] P. Kebarle, U.H. Verkerk, *Mass Spectrom. Rev.*, 28 (2009) 898.
- [55] J.W.S. Rayleigh, *Philos. Mag.*, 14 (1882) 184.
- [56] A. Gomez, K. Tang, *Phys. Fluids*, 6 (1994) 404.

- [57] J.V. Iribarne, B.A. Thomson, *J. Chem. Phys.*, 64 (1976) 2287.
- [58] R. King, R. Bonfiglio, C. Fernandez-Metzler, C. Miller-Stein, T. Olah, *J. Am. Soc. Mass Spectrom.*, 11 (2000) 942.
- [59] J. Sunner, G. Nicol, P. Kebarle, *Anal. Chem.*, 60 (1988) 1300.
- [60] R.R. Loo, N. Dales, P.C. Andrews, *Protein Sci.*, 3 (1994) 1975.
- [61] K.L. Rundlett, D.W. Armstrong, *Anal. Chem.*, 68 (1996) 3493.
- [62] G.W. Somsen, R. Mol, G.J. De Jong, *J. Chromatogr. A*, 1000 (2003) 953.
- [63] G.W. Somsen, R. Mol, G.J. de Jong, *J. Chromatogr. A*, 1217 (2010) 3978.
- [64] J.P. Quirino, P.R. Haddad, *Electrophoresis*, 30 (2009) 1670.
- [65] G. Van Biesen, C.S. Bottaro, *Electrophoresis*, 27 (2006) 4456.
- [66] P. Petersson, M. Jornten-Karlsson, M. Stalebro, *Electrophoresis*, 24 (2003) 999.
- [67] J. Hou, J. Zheng, S.A.A. Rizvi, S.A. Shamsi, *Electrophoresis*, 28 (2007) 1352.
- [68] J. Hou, J. Zheng, S.A. Shamsi, *Electrophoresis*, 28 (2007) 1426.
- [69] S.A.A. Rizvi, J. Zheng, R.P. Apkarian, S.N. Dublin, S.A. Shamsi, *Anal. Chem.*, 79 (2007) 879.
- [70] C.A. Luces, I.M. Warner, *Electrophoresis*, 31 (2010) 1036.
- [71] H. Ozaki, N. Itou, S. Terabe, Y. Takada, M. Sakairi, H. Koizumi, *J. Chromatogr. A*, 716 (1995) 69.
- [72] I.R. Dunkin, A. Gittinger, D.C. Sherrington, P. Whittaker, *J. Chem. Soc., Perkin Trans. 2*, (1996) 1837.
- [73] O. Nuyken, K. Meindl, A. Wokaun, T. Mezger, *J. Photochem. Photobiol., A*, 85 (1995) 291.

- [74] P.E. Hellberg, K. Bergstrom, K. Holmberg, *J. Surfactants Deterg.*, 3 (2000) 81.
- [75] D. Lundberg, M. Stjerndahl, K. Holmberg, *Adv. Polym. Sci.*, 218 (2008) 57.
- [76] A. Tehrani-Bagha, K. Holmberg, *Curr. Opin. Colloid Interface Sci.*, 12 (2007) 81.
- [77] D.A. Jaeger, J. Jamrozik, T.G. Golich, M.W. Clennan, J. Mohebalian, *J. Am. Chem. Soc.*, 111 (1989) 3001.
- [78] E.H. Cordes, H.G. Bull, *Chem. Rev.*, 74 (1974) 581.
- [79] D.A. Jaeger, Y.M. Sayed, A.K. Dutta, *Tetrahedron Lett.*, 31 (1990) 449.
- [80] S. Konig, O. Schmidt, K. Rose, S. Thanos, M. Besselmann, M. Zeller, *Electrophoresis*, 24 (2003) 751.
- [81] S. Yamamura, M. Nakamura, K. Kasai, H. Sato, T. Takeda, *Yukagaku*, 40 (1991) 1002.
- [82] B.E. Root, B. Zhang, A.E. Barron, *Electrophoresis*, 30 (2009) 2117.
- [83] M.S. Li, M.J. Powell, T.T. Razunguzwa, G.A. O'Doherty, *J. Org. Chem.*, 75 (2010) 6149.
- [84] P. Deslongchamps, Y.L. Dory, S. Li, *Tetrahedron*, 56 (2000) 3533.

CHAPTER 2 MICELLAR ELECTROKINETIC CHROMATOGRAPHY WITH ACID LABILE SURFACTANT¹

2.1 INTRODUCTION

Micellar electrokinetic chromatography (MEKC) is a high efficiency separation method that conveniently gives efficiencies greater than 100,000 theoretical plates [1-3]. In MEKC surfactant is present above its critical micelle concentration (CMC). The resultant micelles act as a pseudostationary phase. Analytes that partition into the micelle migrate with an electrophoretic mobility which is a function of both the electrophoretic mobility of the micelle and the partition coefficient [2]. MEKC has been used to separate neutral and charged analytes ranging from small molecules to macromolecules such as peptides, proteins and saccharides [4-12]. MEKC has become a popular separation technique because it gives higher theoretical plate count and consumes less toxic and expensive organic solvent than high performance liquid chromatography (HPLC) [13, 14].

Electrospray ionization mass spectrometry (ESI-MS) is a powerful detection technique, capable of giving rich structural information from aqueous and aqueous/organic solutions [15-17]. ESI-MS' soft ionization enables the transformation of large molecules into gas-phase ions without decomposition [18]. This has made ESI-MS an immensely popular technique to study large

¹ A version of this chapter has been published as "Micellar electrokinetic chromatography with acid labile surfactant", B. Stanley, C.A. Lucy, J. Chromatogr. A, 1226 (2012) 55.

biomolecules. The combination of high efficiency separation and selectivity of MEKC with the versatility of ESI-MS is extremely tempting [19]. However, coupling the two techniques is difficult at best. Low molecular mass surfactants such as sodium dodecyl sulphate (SDS) that are commonly used in MEKC have low volatility, are very surface-active and suppress the analyte signal in the ESI-MS [20]. Some solutions have been developed to circumvent the problem of hyphenating MEKC with ESI-MS [21, 22]. One method is partial-filling MEKC (PF-MEKC) [3, 23, 24]. Briefly, in PF-MEKC there are three plugs inside the capillary. The plugs consist of background electrolyte (BGE), followed by a micellar solution and lastly a sample solution. When voltage is applied, the analytes migrate into the micellar region and are separated. The separated analytes continue to move towards the BGE region that is free of surfactant. The analytes elute out of the capillary and are introduced into an ESI-MS system. The micellar plug is left behind and does not interfere with the ESI-MS analysis. Another method is the use of volatile surfactants such as perfluorooctanoic acid (PFOA). PFOA has low boiling point compared to SDS (190 °C vs. 320 °C). PFOA is volatile enough that it does not concentrate on the surface of the droplets and thereby suppress the analyte ESI-MS signal [25, 26]. Similarly, Goetzinger and Cai employed an organic micellar system of lauric acid and monoamines to couple MEKC with the ESI-MS [27]. Thirdly, high molecular mass surfactants that form polymeric micelles have also been used to unify MEKC with ESI-MS [28-31].

Another potential solution to couple MEKC with ESI-MS is cleavable

surfactants. An example is sodium 4-[(2-methyl-2-undecyl-1,3-dioxolan-4-yl) methoxy]-1-propane sulfonate, also known as acid-labile surfactant (ALS, Fig. 2.1). ALS was introduced in 1999 to replace SDS in PAGE because it has similar denaturing and electrophoretic properties as SDS [32]. ALS can be degraded under acidic condition to give less surface-active products (Fig. 2.1). ALS is available commercially under the name of RapiGest, but the ALS used in this study was synthesized in our lab. ALS has been shown to separate proteins comparably to SDS in a microfluidic electrophoresis device [33]. However, no study of ALS in MEKC of small molecules has been reported.

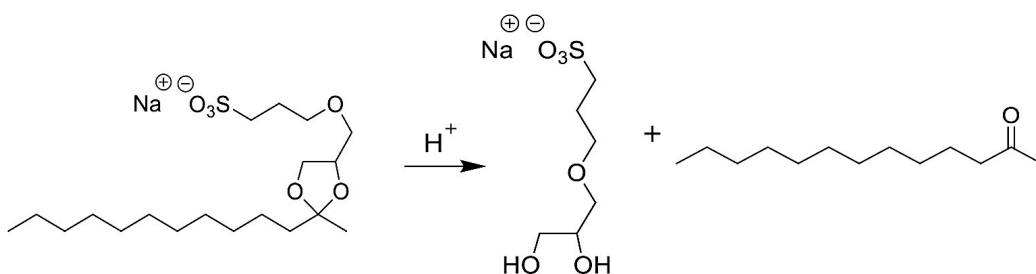


Figure 2.1 Acid hydrolysis of ALS into its less surface-active products

In this work, two aspects of ALS relevant to MEKC-MS are examined. First, ALS is assessed as a pseudostationary phase for MEKC. The micelle mobility, separation efficiency and selectivity of ALS are compared with SDS. Since ALS is degraded under acidic conditions, the stability of the ALS under MEKC conditions is also investigated to ensure that it will be stable during the duration of MEKC separation and analysis. Second, we assess the compatibility of ALS with the ESI-MS. The kinetics of ALS cleavage and the surface activity of the degradation products are determined.

2.2 EXPERIMENTAL

2.2.1 Materials and Reagents

Solutions were prepared with ultrapure (18 M Ω) water (Barnstead, Chicago, IL, USA). The chemicals were of reagent grade or better. 2-Tridecanone, glycerol, *p*-toluenesulfonic acid monohydrate, 1,3-propane sultone, naphthalene, 2-naphthol, anthracene, alkylphenone homologous series (acetophenone – hexanophenone), resorcinol, phenol, 4-nitroaniline, benzyl alcohol, atenolol, disodium tetraborate, sodium phosphate monobasic monohydrate, SDS and formic acid (FA) were used as received from Sigma–Aldrich (Milwaukee, WI, USA). Reagent grade benzene, toluene, ethyl acetate, hexane, methanol, acetonitrile (ACN) and anhydrous ethyl alcohol were from Fisher Scientific (Fairlawn, NJ, USA). The pH of the background electrolyte (BGE) was measured using a Model 445 digital pH meter (Corning, Acton, USA) and were adjusted using 1 M HCl and/or 1 M NaOH. Methanol was used as the EOF marker. All solutions were filtered through 0.2 μ m nylon filters (Barnstead) prior to analyses.

2.2.2 Synthesis of ALS

The synthesis of the ALS precursor 4-hydroxymethyl-2-methyl-2-undecyl-1,3-dioxolane (HMUD) followed that of Jaeger et al. with some modifications [34]. 10 g of 2-tridecanone (0.05 mol), 5.6 g of glycerol (0.06 mol) and 50 mg of *p*-toluenesulfonic acid monohydrate catalyst were dissolved in 250 mL of benzene. The reaction mixture was refluxed with stirring for 45 h in a 500-mL round-bottom flask (RBF) fitted with a Dean-Stark apparatus. The reaction mixture was cooled to room temperature and washed with 500 mL of 5% (m/v) sodium

bicarbonate aqueous solution, dried using Na_2SO_4 and rotary evaporated under vacuum. HMUD is a viscous light yellow liquid. HMUD was purified by flash chromatography (silica, 200–400 mesh, 60 Å; 1:6 v/v ethyl acetate:hexane eluent) before being used in the next step of the synthesis. HMUD was analyzed by a direct injection high resolution ESI-MS, $m/z = 272.42$ (predicted 272.42). The IR spectra of the reaction mixture at the start and the end of the reaction showed the disappearance of the carbonyl peak at 1720 cm^{-1} of 2-tridecanone (Fig. 2.2) and the appearance of hydroxyl peak of HMUD at 3430 cm^{-1} . The yield was 67 – 72%.

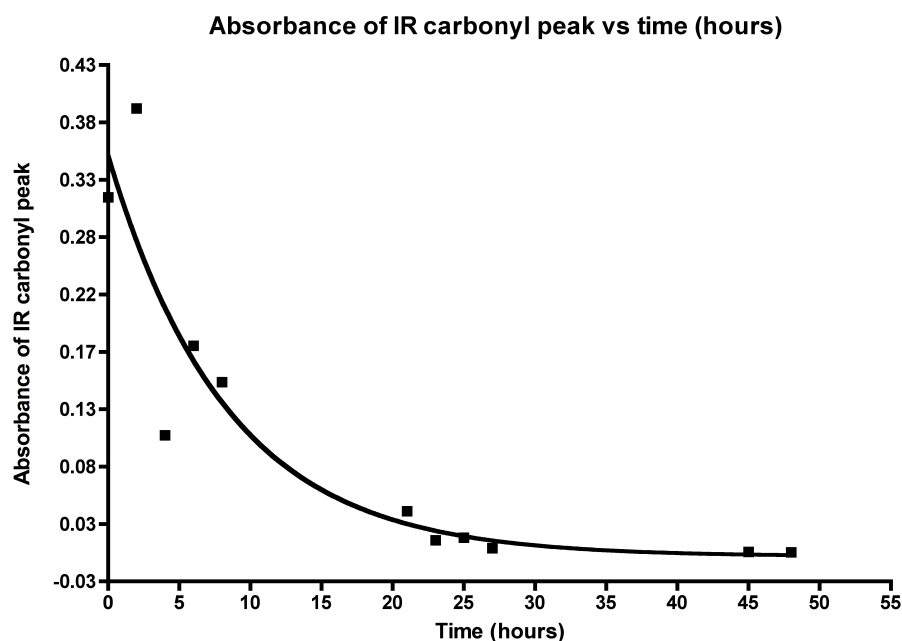


Figure 2.2 Precursor of ALS (HMUD) synthesis monitoring. The rate of disappearance of the carbonyl peak of 2-tridecanone at 1720 cm^{-1} IR (neat film)

The synthesis of ALS from HMUD was performed according to the procedure of Yamamura et al. [35]. Briefly, equimoles of powdered NaOH and HMUD were placed in an RBF with 200 mL of toluene. The mixture was stirred at $50\text{ }^\circ\text{C}$ while equimolar 1,3-propane sultone was added over 30 min. The

suspension was stirred further at 70–75 °C for 6 h. Upon adding the reaction mixture into boiling ethanol, a white precipitate (ALS) formed. The ALS was collected after the removal of the solvent and recrystallized from ethanol. The identity of ALS was confirmed by direct injection high resolution ESI-MS, $m/z = 393.23$ (predicted 393.23). The melting point was 258–262 °C. The yield was 70 – 80%. Solid ALS is stored at 4 °C for future usage. The reaction scheme for the full synthesis of ALS is summarized below in Fig 2.3.

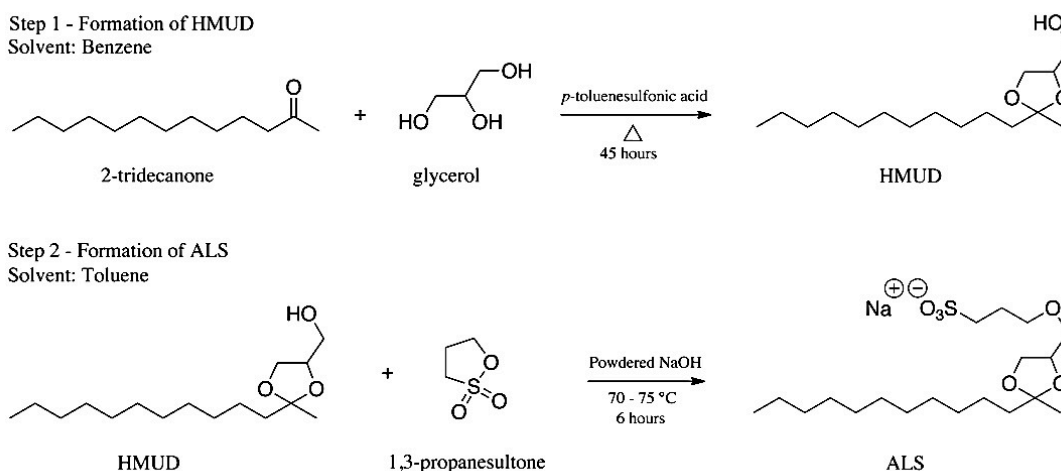


Figure 2.3 Reaction scheme for synthesis of HMUD and ALS.

2.2.3 Instrumentation

MEKC experiments were performed on a Beckman-Coulter P/ACE MDQ system (Fullerton, CA, USA) equipped with a UV absorbance detector monitoring 214 nm. 50 μm ID (363 μm OD) bare fused-silica capillaries (Polymicro Technologies, Phoenix, AZ, USA) with a total length of 51.5 cm and effective length of 41.5 cm were used. The capillary temperature was maintained at 25 °C. New capillaries were flushed with 1.0 M NaOH for 60 min at 20 psi (138 kPa),

followed by 0.1 M NaOH for 30 min at 20 psi (138 kPa). Samples were hydrodynamically injected using 0.3 psi (2.1 kPa) for 3 s. The capillary was rinsed with 0.1 M NaOH for 30 min at the start of each day prior to any analysis. The capillary was flushed with ACN, 0.1 M NaOH and background electrolyte (BGE) respectively for 5 min each at 20 psi (138 kPa) prior to each run.

High resolution ESI-MS analyses were performed on an Agilent Technologies 6220 TOF-ESI-MS (Santa Clara, CA, USA) by direct injection. The cleavage rate study was performed on an Agilent Technologies HP MSD1100 ESI-MS system (Santa Clara, CA, USA) by direct injection. 475 μ L of atenolol (25 mM) dissolved in 0.5% formic acid (FA, pH 2.5) was spiked with 25 μ L of ALS (25 mM) dissolved in deionized water. The solution mixture was homogenized and injected in to the ESI-MS every 30 min for 16 h. Surface tension measurements were taken using a Fisher surface tensiometer model 20 (Fisher Scientific, Pittsburgh, PA). Before each measurement the platinum–iridium ring and 50-mL beaker used were cleaned in benzene.

2.3 RESULTS AND DISCUSSION

2.3.1 Comparison of MEKC with ALS and SDS

SDS is the most widely used surfactant for MEKC separations of both small molecules such as metabolites and macromolecules such as proteins, peptides and saccharides [2, 10, 36-38]. SDS is well characterized, easily available, inexpensive, and highly soluble in aqueous media. It also has a low UV absorbance and high solubilization power.

ALS has a critical micelle concentration (CMC) of 0.5 mM in pure water [35]. This is lower than the 8 mM CMC of SDS [1]. This potentially would allow ALS to be used for MEKC at a lower surfactant concentration, hence avoiding the higher viscosity and conductivity associated with SDS [39]. ALS also has comparable background absorbance as SDS (1.5 vs. 1.6 mAu). These properties make ALS an attractive surfactant to perform MEKC separation.

Fig. 2.4 shows an MEKC separation of six model analytes using ALS. Table 2.1 compares MEKC separations using ALS and SDS in terms of separation efficiency (N) and repeatability. ALS displayed separation efficiencies of 95,000 – 145,000 theoretical plates for more polar analytes ($k' = 0.088 - 0.24$). SDS achieved 110,000 – 180,000 theoretical plates for the same analytes. Separation efficiency decreases for less polar analytes. It ranges from 60,000 – 110,000 for analytes with $k' = 0.7 - 3.1$ in ALS. Theoretical plates of the same analytes using SDS were 55,000 – 150,000.

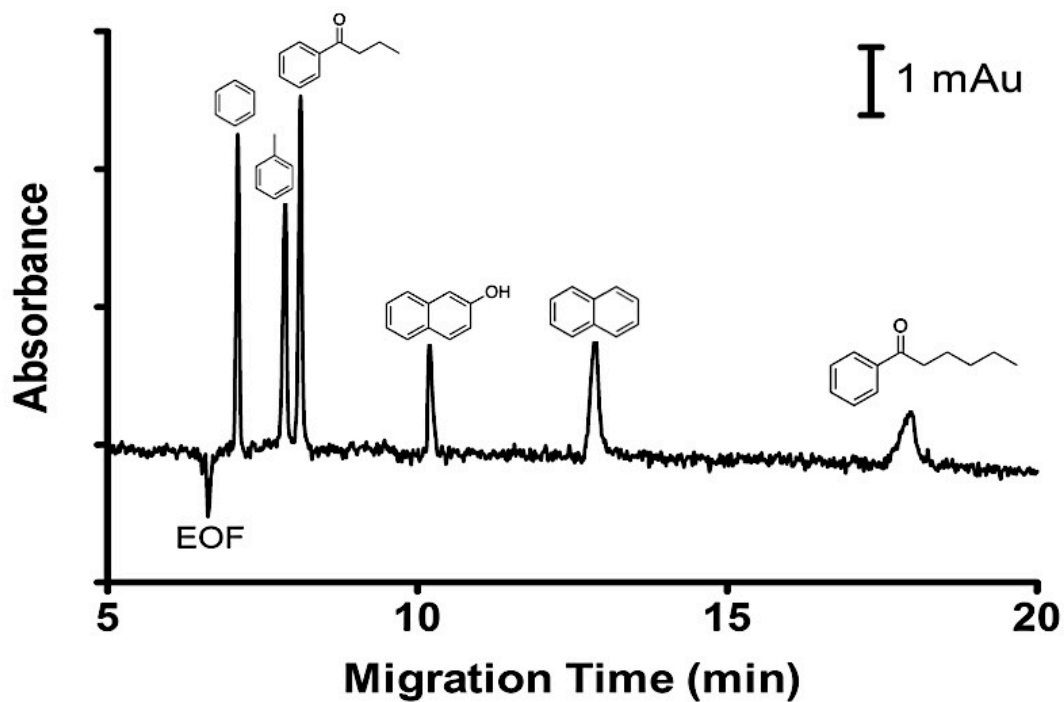


Figure 2.4 Separation of six model analytes using ALS as a pseudostationary phase: benzene, toluene, butyrophenone, 2-naphthol, naphthalene, hexanophenone. Conditions: EOF marker, methanol; detection, 214 nm; applied voltage, 15 kV; BGE, 50 mM NaH_2PO_4 , 100 mM borate, 30 mM ALS, pH 7.04; capillary (50 μm ID) total length, 51.5 cm; effective length, 41.5 cm.

Table 2.1 Comparison of efficiency, repeatability and retention factor (k') between SDS and ALS as a pseudostationary phase.

Analytes	Efficiency SDS	Efficiency ALS	RSD (%) of $\mu_{ep, n}$ = 5, SDS	RSD (%) of $\mu_{ep, n}$ = 5, ALS	k' SDS	k' ALS
Resorcinol	170,000	140,000	1.9	1.3	0.13	0.15
Phenol	175,000	125,000	1.2	1.3	0.26	0.12
Benzyl alcohol	175,000	145,000	0.4	2.0	0.30	0.074
4-nitroaniline	180,000	115,000	1.1	1.2	0.64	0.13
Benzene	145,000	95,000	0.6	2.2	0.84	0.088
Toluene	110,000	105,000	0.2	1.1	1.5	0.24
2-naphthol	95,000	95,000	0.4	0.3	2.8	0.74
Naphthalene	55,000	60,000	0.4	0.5	7.1	1.4
Butyrophenone	150,000	110,000	1.1	1.3	8.6	0.29
Valerophenone	120,000	105,000	0.2	0.9	25.9	0.7
Hexanophenone	90,000	15,000	0.7	0.3	75.5	3.1

Experimental conditions: 50 mM NaH₂PO₄, 100 mM borate, 30 mM surfactant (SDS or ALS), pH 7.04. Detection: 214 nm; total length: 51.5 cm; effective length: 41.5 cm; applied voltage: 15 kV.

Hexanophenone gives surprisingly low peak efficiency (15,000 theoretical plates) for ALS due to peak fronting. This peak shape and the decrease in the peak efficiency are consistent with the non-linear, anti-Langmuir type isotherm observed for hexanophenone in MEKC with latex nanoparticles [40].

Considering other systems to bridge MEKC with the ESI-MS, polymeric micelles [36, 41-44] yield efficiencies up to 600,000 theoretical plates [45] and the volatile surfactant PFOA yields 84,000–89,250 theoretical plates [25]. Thus while ALS provides slightly lower separation efficiency than SDS, ALS can still be considered a good MEKC agent as it gives $N > 100,000$ [1]. ALS also outperforms some other MS compatible systems.

Another important factor in an MEKC pseudostationary phase is the repeatability of the migration time (t_m). SDS is very reliable when it comes to

repeatability. The relative standard deviation (RSD) of the electrophoretic mobility of the 11 model analytes is less than 2% (n = 5) for SDS in Table 2.1. ALS yields comparable electrophoretic mobility repeatability, except for benzyl alcohol and benzene which are slightly higher. Polymeric micelle used with MEKC-ESI-MS analysis showed RSD of 0.8 – 0.9% (n = 3) [46]. The repeatability of ALS is comparable with SDS and polymeric micelle [36]. No repeatability RSD has been reported for volatile surfactants.

Further, ALS is stable under standard (neutral) MEKC conditions. After 8 weeks at room temperature, the net electrophoretic mobility of 4-nitroaniline in 30 mM ALS (pH 7) was equivalent to that of a fresh solution ($-2.22 \times 10^{-5} \text{ cm}^2/\text{V s}$ vs. $-2.07 \times 10^{-5} \text{ cm}^2/\text{V s}$).

2.3.2 Stability of ALS Under Acidic Conditions

ALS is hydrolyzable under acidic conditions [47, 48]. This property is what makes ALS attractive in proteomics because its less surface-active products (Fig. 2.1) are compatible with ESI-MS [32, 49]. While being acid-hydrolyzable is advantageous for ESI-MS detection, ALS needs to be stable over the range of BGE pH used in MEKC. Techniques such as sample stacking with reverse migrating micelle are performed under acidic conditions (pH < 4) to suppress the EOF [50]. ALS must be stable for long enough to be used in such experiment.

To test the stability of ALS, repetitive MEKC separations were performed using 30 mM ALS in pH 4.0 buffer. The net migration time (i.e., observed migration time – migration time of the EOF) of benzyl alcohol is consistent over 60 h (Fig. 2.5), with an RSD of 4.8% and a slope that is statistically equivalent to

zero ($(-5.6 \pm 20) \times 10^{-5}$). These results coupled with those at pH 7 indicate that ALS is hydrolytically stable enough to be used conveniently for MEKC separations.

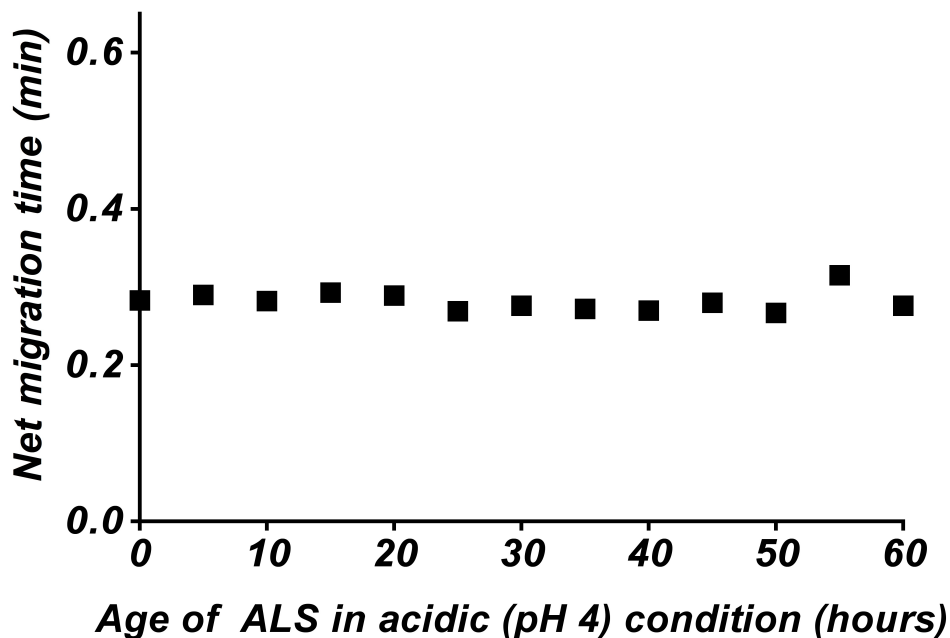


Figure 2.5 Stability plot of ALS for 60 hours. Conditions: Analyte, benzyl alcohol; EOF marker, methanol; detection, 214 nm; applied voltage, 15 kV; BGE, 50 mM NaH_2PO_4 , 100 mM sodium borate, 30 mM ALS, pH 4.00. Capillary: 50 μm ID; total length, 51.5 cm; effective length, 41.5 cm.

2.3.3 Mobility and Selectivity of ALS

As shown in Fig. 1.3, the migration time window for a neutral compound in MEKC is between the migration time of the EOF (t_{eof}) and the micelle (t_{mc}). Common ways to calculate the mobility of the micelle are to use a homologous series or a single marker [51]. The homologous series method was introduced by Bushey and Jorgenson in 1989 [52], and has been used extensively over the years [51]. In this procedure a homologous series (commonly alkylphenones) are separated under MEKC conditions. Initially, the t_m of the compound with the

highest carbon number is assigned as the t_{mc} . The retention factors for the other members of the homologous series are calculated using:

$$k' = \frac{t_m - t_{eof}}{t_{eof} \left[1 - \left(\frac{t_m}{t_{mc}} \right) \right]} \quad (2-1)$$

Ideally a plot of $\log k'$ vs. the carbon number should be linear. If it is not, new $\log k'$ is estimated by extrapolating the regression line to the member of the homologous series with the highest carbon number. The new t_{mc} is calculated by rearranging equation (2-1). The new t_{mc} is used to recalculate the $\log k'$ of each homologous member, which are then again plotted against the carbon number. The process is reiterated until the difference between consecutive values is less than 0.001 min or the correlation coefficient reaches $R^2 = 0.9999$. For MEKC with SDS, the homologous series acetophenone – hexanophenone yielded a linear plot of $\log k'$ vs. carbon number ($R^2 = 0.9999$) and a mobility of SDS micelles of $-3.74 \times 10^{-4} \text{ cm}^2/\text{V s}$. This value is consistent with values reported in the literature for SDS which range from -3.9×10^{-4} to $-4.4 \times 10^{-4} \text{ cm}^2/\text{V s}$ [53, 54].

Unfortunately, attempts to use the homologous series method with ALS resulted in positive deviation of the $\log k'$ vs. carbon number plot and the iterative calculations did not converge. Figure 1.4 displays the positive deviation of the $\log k'$ vs. carbon number plot for an acid-labile surfactant [55]. Although the homologous series has been successfully utilized to determine t_{mc} over the years, there are some cases where it has failed [51, 56, 57]. The failure in ref. [56] displayed a different pattern (i.e. negative deviation) than observed herein, and had been attributed to restricted hydrophobic domains. The other instance of

failure was for a siloxane polymeric micelle [56]. This siloxane polymer contains a similar hydrophilic cyclic-ketal linkage to that in ALS (Fig. 2.1). None of the pseudostationary phases for which the homologous series method has been successful contain such a polar linker [51]. However, more investigations need to be done before any concrete conclusion can be reached.

In the single-marker method, a hydrophobic compound that is fully partitioned into the pseudostationary phase is used to calculate the electrophoretic mobility of the pseudostationary phase. Compounds that have been used as micelle markers include Sudan III, dodecanophenone, anthracene and decanophenone [4, 51, 57, 58]. Using anthracene with SDS yielded a micelle mobility of $-3.70 \times 10^{-4} \text{ cm}^2/\text{V s}$, in excellent agreement with the value determined using the homologous series method ($-3.74 \times 10^{-4} \text{ cm}^2/\text{V s}$). The mobility of ALS micelles based on anthracene is $-2.33 \times 10^{-4} \text{ cm}^2/\text{V s}$. The elution window in MEKC is determined by the EOF and the micelle mobility. Faster micelle mobility results in greater elution window and hence larger peak capacity. The migration window time ratios (t_{mc}/t_{eof}) of ALS and SDS are 6.6 and 9.5 respectively. This shows that ALS has a smaller migration window time ratio than SDS. ALS has slower mobility compared to polymeric micelles such as sodium 10-undecenyl sulphate ($-4.3 \times 10^{-4} \text{ cm}^2/\text{V s}$) and siloxane polymer ($-5.3 \times 10^{-4} \text{ cm}^2/\text{V s}$) [44, 59]. However, the ALS mobility does fall within the range of common pseudostationary phases (-2.35 to $-5.3 \times 10^{-4} \text{ cm}^2/\text{V s}$) [59].

Both the hydrophilic and hydrophobic groups determine the selectivity of a surfactant in MEKC. ALS has a similar hydrophobic tail as SDS, but a different

palisade region. Thus we expect ALS to offer different selectivity. Fig. 2.6 shows the log of retention factor (k') of eleven different analytes using ALS and SDS as the pseudostationary phase. Retention factors with ALS are strongly correlated with those with SDS, as evidenced by the R^2 of 0.79 for the eleven analytes in Fig. 2.6, and an $R^2 = 0.992$ for specifically the non-hydrogen bonding (NHB) analytes. However, ALS displays different selectivity than SDS for hydrogen bond donor (HBD) and hydrogen bond acceptor (HBA) compounds (R^2 of 0.74 and 0.88, respectively). The HBD solutes show higher affinity for ALS (top line) whereas the HBA solutes have higher affinity for SDS (bottom line). This behavior is similar to what was observed in the selectivity comparison between lithium perfluorooctanesulfonate (LiPFOS) and SDS, where the hydrophobic interaction is the primary driving force between micelle–solute interactions [60].

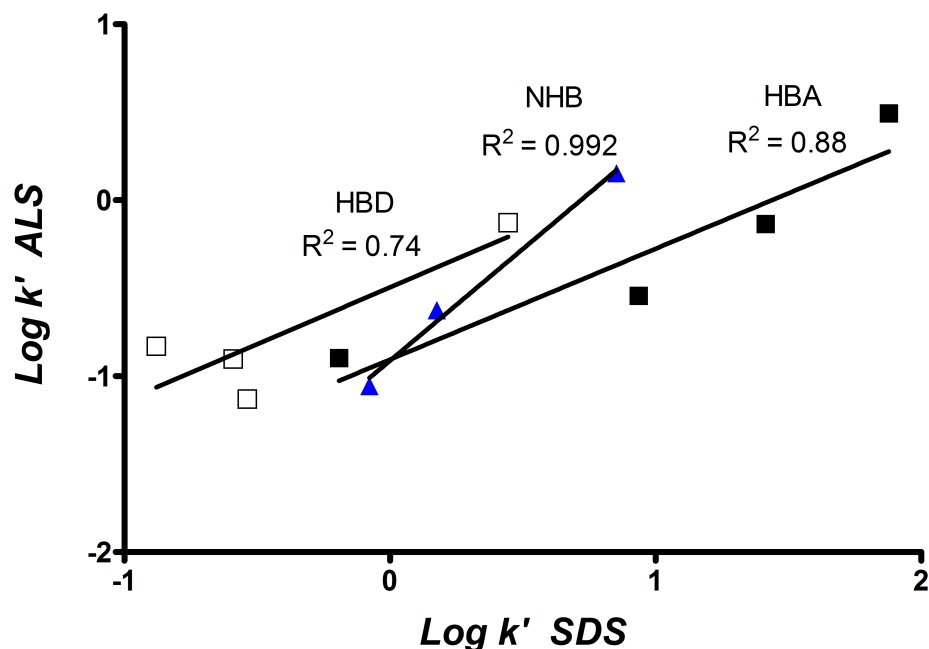


Figure 2.6 Log k' of eleven analytes using ALS and SDS as pseudostationary phase. □ = hydrogen bond donating (resorcinol, phenol, benzyl alcohol, 2-naphthol), $R^2 = 0.74$; ■ = hydrogen bond acceptor (4-nitroaniline, butyrophenone, valerophenone, hexanophenone), $R^2 = 0.88$; ▲ = non-hydrogen bonding (benzene, toluene, naphthalene), $R^2 = 0.992$. Conditions: EOF marker, methanol; detection, 214 nm; applied voltage, 15 kV; BGE, 50 mM NaH_2PO_4 , 100 mM sodium borate, 30 mM ALS or SDS, pH 7.04.

The k' of hydrophobic analytes with ALS are much lower than with SDS (Table 2.1). For example, the k' of naphthalene is 1.4 and 7.1 using 30 mM ALS and SDS respectively. As a result of this lower retention, ALS resolves hydrophobic analytes well (Fig. 2.4). However, ALS is at a disadvantage in separating hydrophilic analytes, whose retention becomes too low to affect separation. For instance, SDS resolves resorcinol and 4-nitroaniline ($k' = 0.13$ and 0.64 respectively) whereas ALS does not ($k' = 0.15$ and 0.13 respectively).

2.3.4 Cleavage Rate of ALS and Compatibility with ESI-MS

There are two requirements that ALS needs to fulfill before it can link MEKC with online ESI-MS. First, ALS must decompose into less surface-active

compounds. Second, the hydrolysis of ALS should be as rapid as possible. Preliminary studies monitored the hydrolysis via surface tension. The surface tension of a 25 mM ALS (pH 7) solution was measured as 46 dynes/cm, which is in good agreement with the literature (41 dynes/cm) [35]. After 19 h hydrolysis with 0.5% formic acid, the surface tension increased to 58 dynes/cm. The surface tension right after the addition of 0.5% formic acid was 30.5 dynes/cm ($n = 3$). This shows that the increase in surface tension is due to hydrolysis of ALS and not to the presence of formic acid.

To more directly study the effect of ALS on ESI-MS, the ESI-MS signal of atenolol as a model analyte was monitored. The m/z of atenolol (311.2) is easily resolved from that of ALS (393.2). Prior to hydrolysis (time = 0), the ALS dominates the ESI signal (Fig. 2.7) of an equimolar solution of ALS and atenolol. With degradation of the ALS (e.g., 16 h in Fig. 2.7), the atenolol signal increases. As a control, the same experiment using SDS showed that SDS signal still dominates over the atenolol signal after 16 h (Fig. 2.8). To monitor the hydrolysis kinetics, the ESI signal intensity ratio of ALS over atenolol was plotted vs. time (Fig. 2.9). The half-life of ALS hydrolysis is 48 min at pH 2.5 in water. Alternately the half-life of ALS in a 50/50 ACN/0.5% FA solution is 170 min (Fig. 2.10). Fig. 2.7 and 2.9 confirm that the degradation products of ALS are less surface-active than the original ALS, consistent with literature claims [32, 33]. Unfortunately, the long half-life of ALS makes online coupling of MEKC-ESI-MS unrealistic. However, the high separation efficiency and selectivity of ALS make it attractive for MEKC-fraction collection mass spectrometry [61, 62].

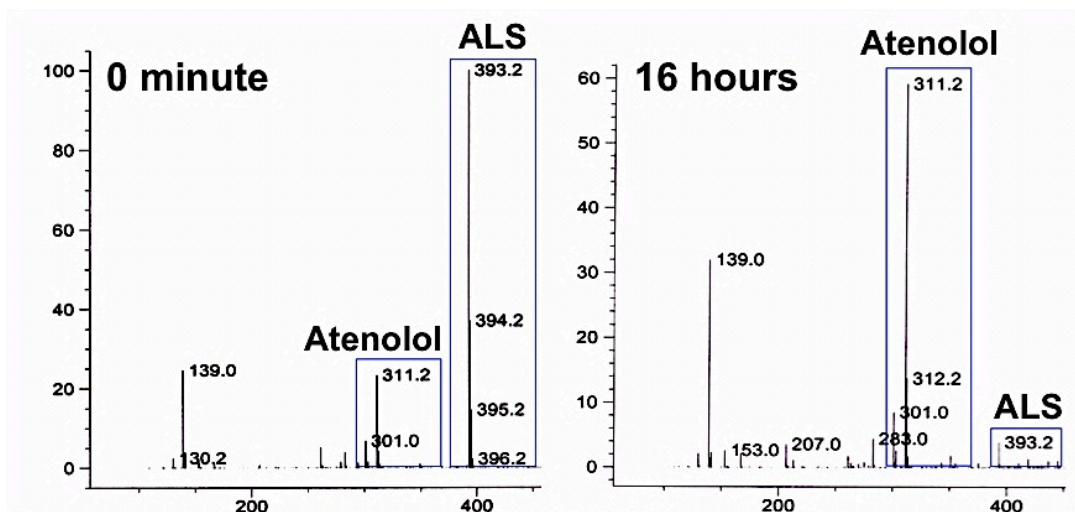


Figure 2.7 Mass spectra of atenolol and ALS at 0 minute and 16 hours. Conditions: 475 μL of atenolol (25 mM in 0.5% formic acid) spiked with 25 μL of ALS (25 mM in deionized water). Conditions: negative mode; fragmentation energy, 80 V; solvent system, methanol. Atenolol peak is $[\text{M}+\text{FA}-\text{H}]^-$. ALS peak is $[\text{M}]^-$.

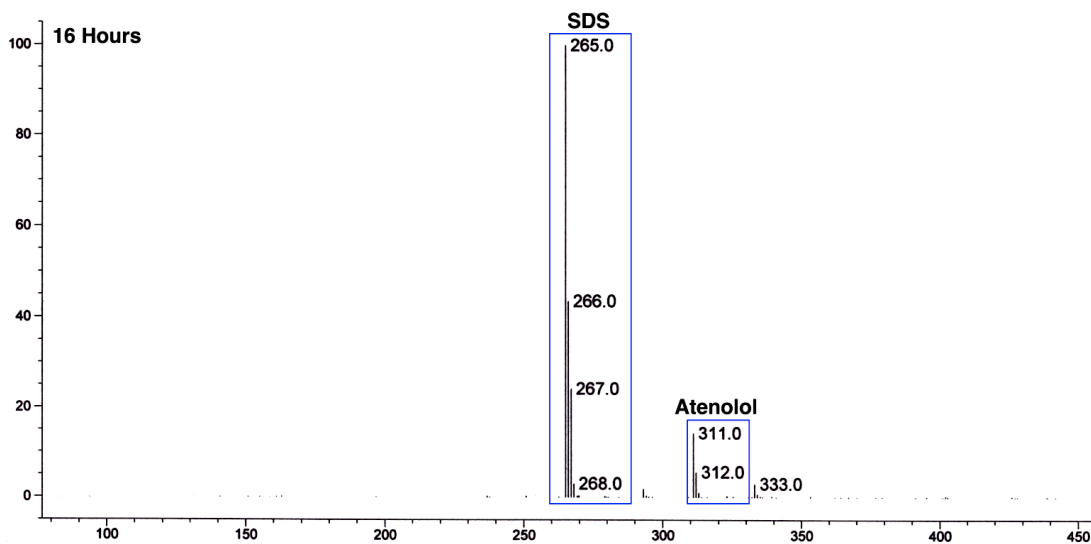


Figure 2.8 Mass spectrum of atenolol and SDS at 16 hours. Conditions: 475 μL of atenolol (25 mM in 0.5% formic acid) spiked with 25 μL of SDS (25 mM in deionized water). Conditions: negative mode; fragmentation energy, 80 V; solvent system, methanol. Atenolol peak is $[\text{M}+\text{FA}-\text{H}]^-$. SDS peak is $[\text{M}]^-$.

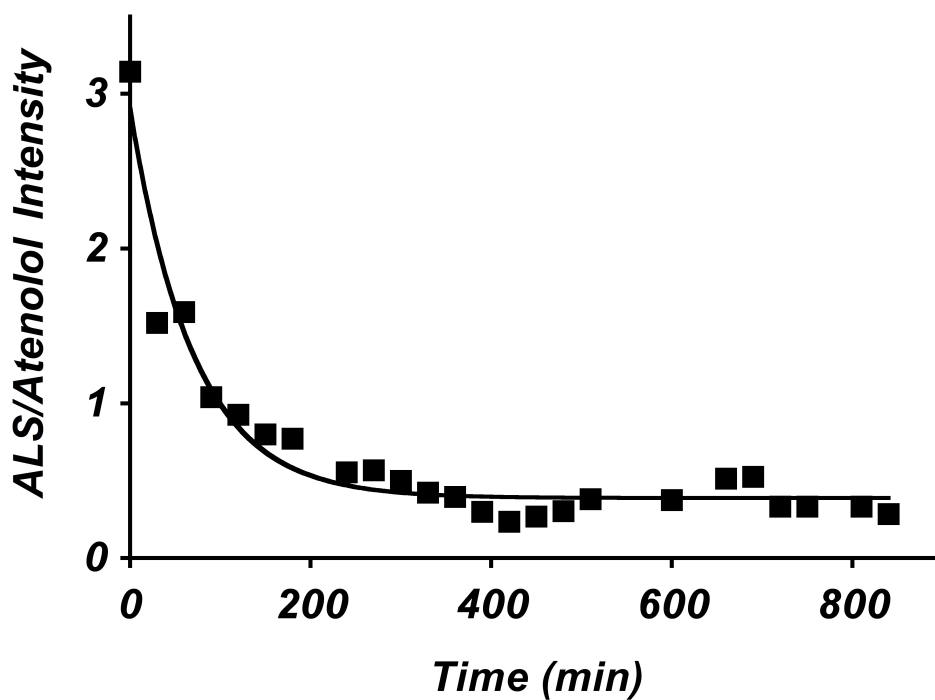


Figure 2.9 Ratio of ALS/atenolol ESI-MS signal intensity over a period of 16 hours in H₂O. Conditions: 475 μ L of atenolol (25 mM in 0.5% formic acid), pH 2.5, spiked with 25 μ L of ALS (25 mM in deionized water). Conditions: fragmentation energy, 80 V; solvent system, methanol; Half-life of ALS, 48 min.

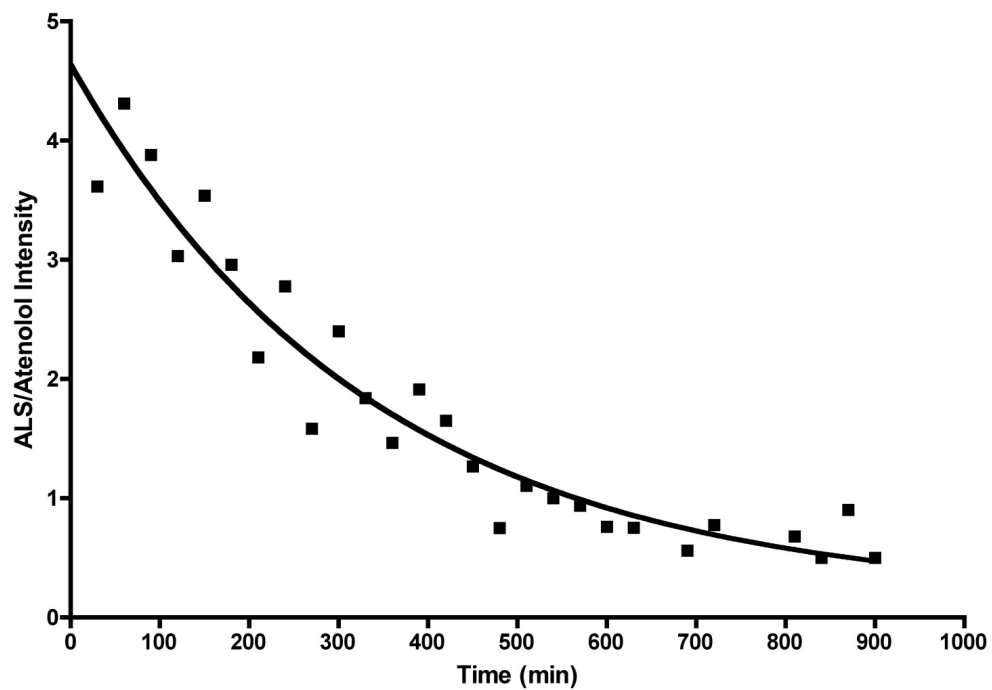


Figure 2.10 Ratio of ALS/atenolol ESI-MS signal intensity over a period of 16 hours in 50% ACN/H₂O. Conditions: 475 μ L of atenolol (25 mM in 50/50 ACN/0.5% formic acid), pH 2.5, spiked with 25 μ L of ALS (25 mM in 50/50 ACN/0.5% formic acid). Conditions: fragmentation energy, 80 V; solvent system, methanol; Half-life of ALS, 170 min.

2.4 CONCLUDING REMARKS

The acid labile surfactant sodium 4-[(2-methyl-2-undecyl-1,3-dioxolan-4-yl) methoxy]-1-propane sulfonate (ALS) was used as pseudostationary phase for high efficiency MEKC separation for the first time. ALS achieved separation efficiency slightly lower than that achieved with SDS, but greater than that of alternate ESI friendly pseudostationary phase. ALS is stable for a reasonable period of time even under acidic condition allowing its usage as a pseudostationary phase. ALS also offers a different selectivity than SDS. ALS is acid hydrolyzed into less surface-active compounds that are more compatible with the ESI-MS. However, the slow cleavage rate of ALS restricts its use to offline MEKC-ESI-MS system.

2.5 REFERENCES

- [1] S. Terabe, *Anal. Chem.*, 76 (2004) 240A.
- [2] S. Terabe, *Chem. Rec.*, 8 (2008) 291.
- [3] M. Silva, *Electrophoresis*, 32 (2011) 149.
- [4] S. Terabe, K. Otsuka, K. Ichikawa, A. Tsuchiya, T. Ando, *Anal. Chem.*, 56 (1984) 111.
- [5] H. Nishi, T. Fukuyama, S. Terabe, *J. Chromatogr.*, 553 (1991) 503.
- [6] H. Shadpour, S.A. Soper, *Anal. Chem.*, 78 (2006) 3519.
- [7] G.T. Roman, K. McDaniel, C.T. Culbertson, *Analyst*, 131 (2006) 194.
- [8] J.M. Sanchez, V. Salvado, *J. Chromatogr. A*, 950 (2002) 241.
- [9] B. Stanley, K.A. Mehr, T. Kellock, J.D. Van Hamme, K.K. Donkor, *J. Sep. Sci.*, 32 (2009) 2993.
- [10] P.J. Oefner, C. Chiesa, *Glycobiology*, 4 (1994) 397.
- [11] Z. El Rassi, *Electrophoresis*, 31 (2010) 174.
- [12] V. Kašička, *Electrophoresis*, 31 (2010) 122.
- [13] M. Silva, *Electrophoresis*, 28 (2007) 174.
- [14] S. Terabe, *Annu. Rev. Anal. Chem.*, 2 (2009) 99.
- [15] J.B. Fenn, M. Mann, C.K. Meng, S.F. Wong, C.M. Whitehouse, *Mass Spectrom. Rev.*, 9 (1990) 37.
- [16] R.D. Smith, J.A. Loo, C.G. Edmonds, C.J. Barinaga, H.R. Udseth, *Anal. Chem.*, 62 (1990) 882.
- [17] H. Stutz, *Electrophoresis*, 26 (2005) 1254.

- [18] J.B. Fenn, M. Mann, C.K. Meng, S.F. Wong, C.M. Whitehouse, *Science*, 246 (1989) 64.
- [19] C.W. Klampfl, *Electrophoresis*, 30 (2009) S83.
- [20] K.L. Rundlett, D.W. Armstrong, *Anal. Chem.*, 68 (1996) 3493.
- [21] G.W. Somsen, R. Mol, G.J. de Jong, *J. Chromatogr. A*, 1217 (2010) 3978.
- [22] G.W. Somsen, R. Mol, G.J. De Jong, *J. Chromatogr. A*, 1000 (2003) 953.
- [23] W.M. Nelson, Q. Tang, A.K. Harrata, C.S. Lee, *J. Chromatogr. A*, 749 (1996) 219.
- [24] J.P. Quirino, P.R. Haddad, *Electrophoresis*, 30 (2009) 1670.
- [25] P. Petersson, M. Jornten-Karlsson, M. Stalebro, *Electrophoresis*, 24 (2003) 999.
- [26] G. Van Biesen, C.S. Bottaro, *Electrophoresis*, 27 (2006) 4456.
- [27] W.K. Goetzinger, H. Cai, *J. Chromatogr. A*, 1079 (2005) 372.
- [28] J. Hou, J. Zheng, S.A.A. Rizvi, S.A. Shamsi, *Electrophoresis*, 28 (2007) 1352.
- [29] J. Hou, J. Zheng, S.A. Shamsi, *Electrophoresis*, 28 (2007) 1426.
- [30] S.A.A. Rizvi, J. Zheng, R.P. Apkarian, S.N. Dublin, S.A. Shamsi, *Anal. Chem.*, 79 (2007) 879.
- [31] M. Silva, *Electrophoresis*, 30 (2009) 50.
- [32] S. Konig, O. Schmidt, K. Rose, S. Thanos, M. Besselmann, M. Zeller, *Electrophoresis*, 24 (2003) 751.
- [33] B.E. Root, B. Zhang, A.E. Barron, *Electrophoresis*, 30 (2009) 2117.
- [34] D.A. Jaeger, J. Jamrozik, T.G. Golich, M.W. Clennan, J. Mohebalian, *J. Am. Chem. Soc.*, 111 (1989) 3001.

- [35] S. Yamamura, M. Nakamura, K. Kasai, H. Sato, T. Takeda, *Yukagaku*, 40 (1991) 1002.
- [36] S.A. Shamsi, B.E. Miller, *Electrophoresis*, 25 (2004) 3927.
- [37] F.A. Tomas-Barberan, *Phytochem. Anal.*, 6 (1995) 177.
- [38] H. Watzig, M. Degenhardt, A. Kunkel, *Electrophoresis*, 19 (1998) 2695.
- [39] M.G. Khaledi, *J. Chromatogr. A*, 780 (1997) 3.
- [40] C.P. Palmer, E.F. Hilder, J.P. Quirino, P.R. Haddad, *Anal. Chem.*, 82 (2010) 4046.
- [41] F. Haddadian, S.A. Shamsi, I.M. Warner, *Electrophoresis*, 20 (1999) 3011.
- [42] C.A. Luces, S.O. Fakayode, M. Lowry, I.M. Warner, *Electrophoresis*, 29 (2008) 889.
- [43] C.A. Luces, I.M. Warner, *Electrophoresis*, 31 (2010) 1036.
- [44] C.P. Palmer, *J. Chromatogr. A*, 780 (1997) 75.
- [45] C. Akbay, S.A.A. Rizvi, S.A. Shamsi, *Anal. Chem.*, 77 (2005) 1672.
- [46] D. Norton, S.A. Shamsi, *Anal. Chem.*, 79 (2007) 9459.
- [47] P.E. Hellberg, K. Bergstrom, K. Holmberg, *J. Surfactants Deterg.*, 3 (2000) 81.
- [48] D. Lundberg, M. Stjerndahl, K. Holmberg, *Adv. Polym. Sci.*, 218 (2008) 57.
- [49] M. Zeller, E.K. Brown, E.S.P. Bouvier, S. Konig, *J. Biomol. Technol.*, 13 (2002) 1.
- [50] J.P. Quirino, S. Terabe, *Anal. Chem.*, 70 (1998) 149.
- [51] S.K. Wiedmer, J. Lokajova, M.L. Riekkola, *J. Sep. Sci.*, 33 (2010) 394.
- [52] M.M. Bushey, J.W. Jorgenson, *Anal. Chem.*, 61 (1989) 491.

- [53] P.G. Muijselaar, M.A. Van Straten, H.A. Claessens, C.A. Cramers, J. Chromatogr. A, 766 (1997) 187.
- [54] E.S. Ahuja, E.L. Little, K.R. Nielsen, J.P. Foley, Anal. Chem., 67 (1995) 26.
- [55] B. Stanley, C.A. Lucy, J. Chromatogr. A, 1226 (2012) 55.
- [56] D.S. Peterson, C.P. Palmer, Electrophoresis, 22 (2001) 1314.
- [57] C.P. Palmer, N. Tanaka, J. Chromatogr. A, 792 (1997) 105.
- [58] P. Morin, J.C. Archambault, P. Andre, M. Dreux, E. Gaydou, J. Chromatogr. A, 791 (1997) 289.
- [59] E. Fuguet, C. Ràfols, E. Bosch, M. Rosés, Electrophoresis, 23 (2002) 56.
- [60] S. Yang, M.G. Khaledi, Anal. Chem., 67 (1995) 499.
- [61] M.M. Yassine, N. Guo, H. Zhong, L. Li, C.A. Lucy, Anal. Chim. Acta., 597 (2007) 41.
- [62] H. Zhang, C. Zhang, G.A. Lajoie, K.K.C. Yeung, Anal. Chem., 77 (2005) 6078.

CHAPTER 3 MICELLAR ELECTROKINETIC CHROMATOGRAPHY AND ELECTROSPRAY IONIZATION MASS SPECTROMETRY WITH AN ACYCLIC KETAL-CONTAINING SURFACTANT**

3.1 INTRODUCTION

Electrospray ionization mass spectrometry (ESI-MS) is a powerful qualitative and quantitative analytical detector. ESI-MS is a soft ionization technique that is able to transform large molecules such as peptides and proteins into gas-phase ions without decomposing them in the process [1]. ESI-MS is also capable of giving rich structural data from aqueous and aqueous/organic solutions [2, 3]. These two abilities have made ESI-MS a very powerful and versatile detection technique. However, ESI-MS is prone to ion-suppression effect that can come from sample matrix and co-eluting analytes [4, 5]. Ion-suppression effects reduce the analyte signal and increase the limit of detection (LOD). A high efficiency separation prior to the ESI-MS analysis can reduce ion-suppression effect caused by the matrix. One example of a high efficiency separation technique is micellar electrokinetic chromatography (MEKC).

MEKC is a mode of separation for capillary electrophoresis (CE). MEKC is a high efficiency separation method that gives >100,000 theoretical plates [6-10]. Surfactants form micelles above these critical micelle concentration. These micelles serve as a pseudostationary phase in an MEKC separation. Analytes

** I initiated the project, and performed all MEKC and all non-synthetic experiments. OALS synthesis was performed by Bing Bai.

partition into the micelle and spend time both inside the micelle and the bulk solution. The electrophoretic mobility of the micelle is a function of the electrophoretic mobility of the micelle and the distribution coefficient [9]. MEKC has been used to separate neutral and charged analytes such as small molecules, amino acids, peptides, proteins and saccharides [6, 11-14]. MEKC has become a popular separation technique because not only it harnesses the high efficiency of CE, but also consumes much less toxic and expensive organic solvents [9, 15].

Hyphenating MEKC and ESI-MS will take advantage of high efficiency and selectivity of MEKC together with the versatility of ESI-MS [16]. However, coupling the two techniques is difficult [17]. The surfactant used in MEKC is very surface-active and causes ion-suppression in ESI-MS [18]. It has been recorded in the literature that as little as 1.25 mM of the anionic surfactant sodium dodecyl sulphate (SDS) suppressed the analyte ion ESI-MS signal [18]. That demonstrates that low molecular weight surfactants are not compatible with ESI-MS [5]. Some ways have been developed to link MEKC with ESI-MS were discussed in Section 2.1. As demonstrated in Chapter 2 [19] one of the potential solutions is the use of an acid-labile surfactant that contains a ketal linkage.

A ketal is a product of reaction between alcohol and ketone (Fig. 1.9). The formation of ketal is reversible and ketal can be acid-hydrolyzed back into ketone and alcohol [20]. Ketals may be either cyclic or acyclic. Sodium 4-[(2-methyl-2-undecyl-1,3-dioxolan-4-yl) methoxy]-1-propane sulfonate (ALS) is an example of a cyclic ketal. In Chapter 2 I demonstrated that ALS can be used to perform MEKC separations. The hydrolysis products of ALS are compatible with ESI-MS

[19]. However, the half-life of ALS was too long for it to be compatible with online MEKC-ESI-MS. Cyclic-ketal is more stable than its acyclic counterpart [20, 21]. Therefore, a surfactant that contains an acyclic-ketal linkage in the palisade region should hydrolyze faster [22]. Sodium 2,2-Bis(hexyloxy)propyl sulphate (OALS) is a recently developed surfactant with an acyclic-ketal linkage [22] (Fig. 3.1). The faster hydrolysis rate makes OALS attractive as an alternative to ALS to hyphenate MEKC with ESI-MS.

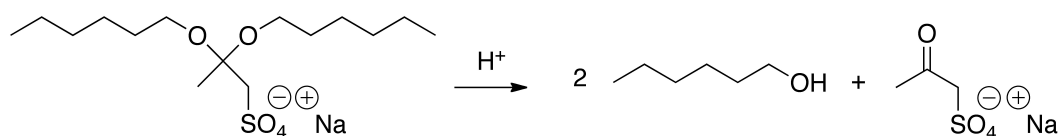


Figure 3.1 Acid hydrolysis of OALS.

In this chapter, the performance of OALS as a pseudostationary phase is assessed. The micelle mobility and selectivity of OALS are compared with SDS and ALS. OALS degrades much faster than ALS. Therefore, the use of temperature and pH to control the hydrolysis rate of OALS are investigated. The compatibility of OALS prior to and after hydrolysis with the ESI-MS is investigated. The kinetics of OALS is also determined.

3.2 EXPERIMENTAL

3.2.1 Materials and Reagents

Solutions were prepared with ultrapure (18 MΩ) water (Barnstead, Chicago, IL, USA). The chemicals were of reagent grade or better. Naphthalene, 2-methylnaphthalene, 2-naphthol, alkylphenone homologous series (acetophenone

– hexanophenone), resorcinol, phenol, aniline, 4-nitroaniline, tryptophan, ammonium acetate, SDS, acetic acid and formic acid (FA) were used as received from Sigma–Aldrich (Milwaukee, WI, USA). Reagent grade benzene, toluene, ethyl acetate, hexane and methanol were from Fisher Scientific (Fairlawn, NJ, USA). The pH of the background electrolyte (BGE) was measured using a Model 445 digital pH meter (Corning, Acton, USA) and were adjusted using 1 M acetic acid and/or 3% v/v NH₄OH. Methanol was used as the EOF marker. All solutions were filtered through 0.2 μm nylon filters (Barnstead) prior to analyses.

3.2.2 Synthesis of OALS

The synthesis of sodium 2,2-Bis(hexyloxy)propyl sulphate (OALS) consists of five steps, as shown in Figure 3.2. Our yields for each step are reported in Figure 3.2. The synthesis followed the method outlined by Li and colleagues except for the purification of the final product in step 5 [22]. After the fifth reaction was completed, the solvent was removed by rotovaporation and the residue (OALS and salt impurity) was dissolved in hexane. The salt impurity was insoluble in hexane and removed by filtration. The procedure was repeated till there is no more residue present. The hexane was removed by rotovaporation to give yellow pure product (OALS). The identity of OALS was confirmed by direct injection high resolution ESI-MS, $m/z = 339.1846$; predicted 339.1847 (see Figure 3.3).

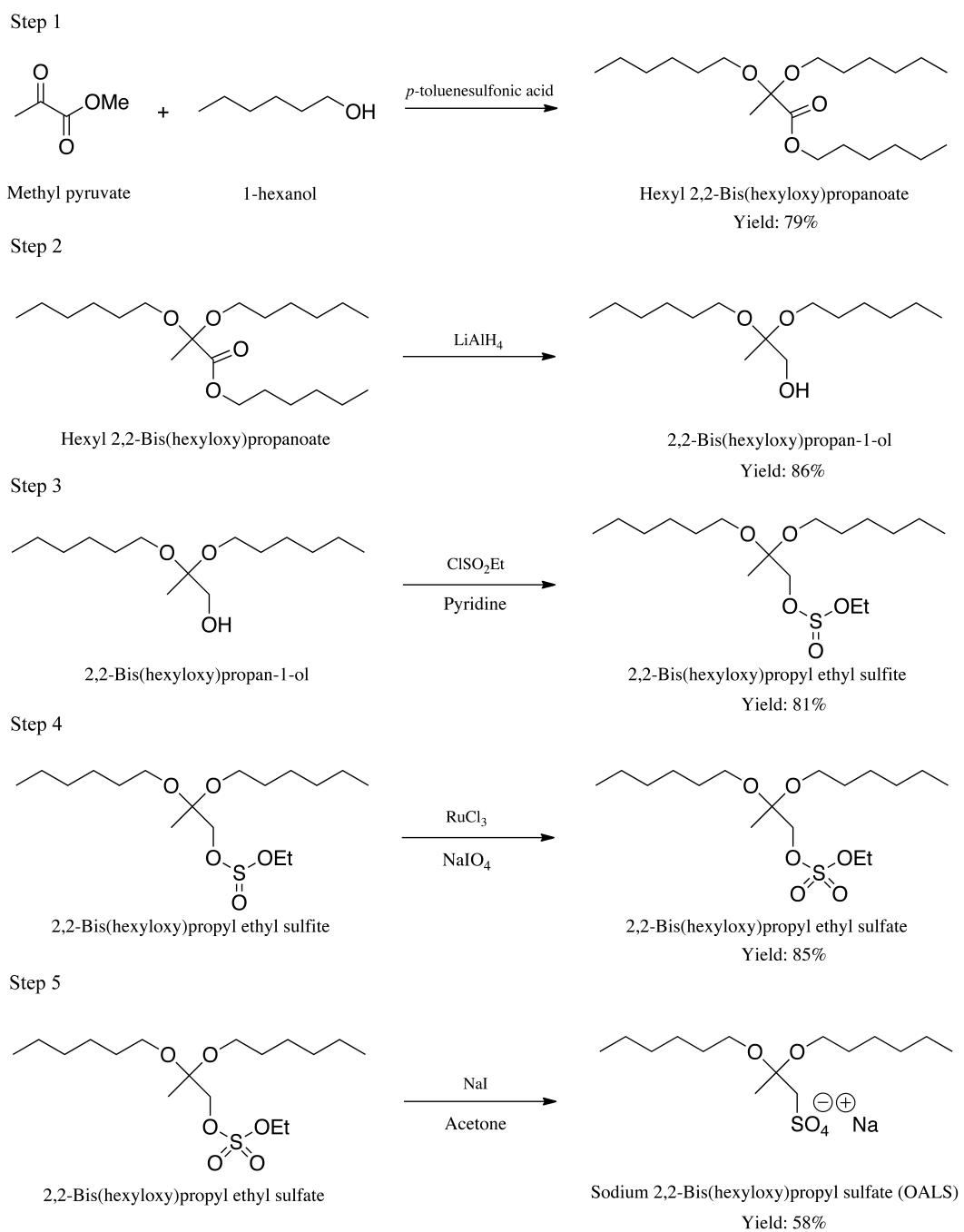


Figure 3.2 Reaction scheme for the five-step synthesis of sodium 2,2-Bis(hexyloxy)propyl sulphate (OALS). Adapted from [22].

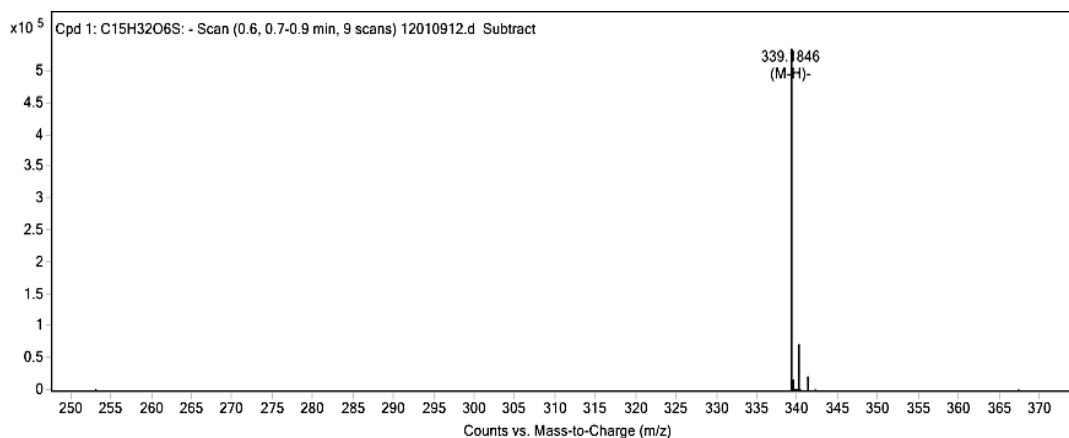


Figure 3.3 High resolution ESI-MS mass spectrum of OALS, $m/z = 339.1846$ (predicted 339.1847).

3.2.3 Instrumentation

MEKC experiments were performed on a Beckman-Coulter P/ACE MDQ system (Fullerton, CA, USA) equipped with a UV absorbance detector monitoring 214 nm. 50 μm ID (363 μm OD) bare fused-silica capillaries (Polymicro Technologies, Phoenix, AZ, USA) with a total length of 51.5 cm and effective length of 41.5 cm were used. The capillary temperature was maintained at 25 $^{\circ}\text{C}$ unless otherwise noted. New capillaries were flushed with 1.0 M NaOH for 60 min at 20 psi (138 kPa), followed by 0.1 M NaOH for 30 min at 20 psi (138 kPa). The capillary was flushed with 3% v/v NH_4OH and background electrolyte (BGE) respectively for 5 min each at 20 psi (138 kPa) prior to each run. Samples were hydrodynamically injected using 0.3 psi (2.1 kPa) for 3 s. The capillary was rinsed with 3% v/v NH_4OH for 30 min at the start of each day prior to any analysis.

High resolution ESI-MS analyses were performed on an Agilent Technologies 6220 TOF ESI-MS (Santa Clara, CA, USA) by direct injection. The cleavage rate study was performed on an Agilent Technologies HP MSD1100

ESI-MS system (Santa Clara, CA, USA) by direct injection. 475 μL of tryptophan (25 mM) dissolved in 0.5% formic acid (FA, pH 2.5) or 5 mM ammonium acetate (pH 4.50) was spiked with 25 μL of OALS (25 mM) dissolved in deionized water. The solution mixture was homogenized and injected in to the ESI-MS every minute for 20 min.

3.3 RESULTS AND DISCUSSION

3.3.1 Mobility and Selectivity of OALS

The type of surfactant plays a significant role in MEKC [23-25]. The chemical composition of the hydrophobic tail and ionic head group in a surfactant determine the selectivity factor and the mobility of the micelles. These influence the three factors affecting resolution in MEKC, i.e. retention factor (k'), selectivity and the migration time window (t_{mc}/t_{eof}) as expressed in equation 1-4 [8, 24].

SDS is the most widely used surfactant for MEKC separations [9, 10]. As shown in Figure 1.3, the width of the t_{mc}/t_{eof} window is directly proportional with the mobility of the micelle. The mobility of SDS ranges from -3.7×10^{-4} to $-4.4 \times 10^{-4} \text{ cm}^2/\text{V s}$ [26, 27]. Herein, the mobility of SDS was determined using the alkylphenone homologous series [28], as discussed in detail in Section 1.2.3.2. The observed mobility of SDS is $-3.70 \pm 0.06 \times 10^{-4} \text{ cm}^2/\text{V s}$ in 50 mM ammonium acetate buffer, in excellent agreement with the literature. The high SDS mobility is an advantage because it gives a wide t_{mc}/t_{eof} [19, 26, 29]. The alkylphenone homologous series was then used to measure the mobility of OALS.

Unlike the experience with ALS (Chapter 2), the homologous series method yielded an excellent linearity ($R^2 = 0.9999$) for a plot (Fig. 3.4) of $\log k'$ vs. carbon number for OALS. The mobility of OALS is $-4.20 \pm 0.04 \times 10^{-4} \text{ cm}^2/\text{V s}$. Thus, OALS has greater mobility than SDS, which means OALS gives a wider t_{mc}/t_{eof} and thus potentially greater peak capacity. The OALS mobility is also substantially greater than the mobility of another cleavable surfactant ALS (Section 2.3.3, [19])

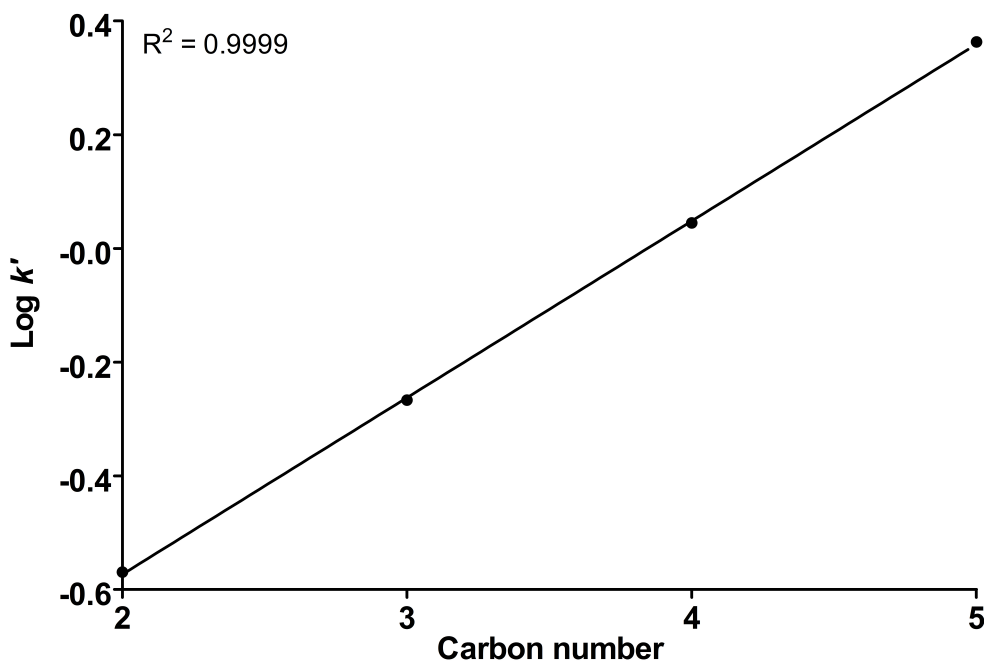


Figure 3.4 Plot of $\text{Log } k'$ vs. Carbon number of the alkylphenones homologous series (acetophenone – valerophenone). Conditions: EOF marker, methanol; detection, 214 nm; applied voltage, 15 kV; BGE, 50 mM ammonium acetate, 30 mM OALS, pH 9.00.

In term of selectivity, the OALS is compared with both SDS and sodium 4-[(2-methyl-2-undecyl-1,3-dioxolan-4-yl) methoxy]-1-propane sulfonate (ALS) using hydrogen bond donor (HBD), hydrogen bond acceptor (HBA) and non-hydrogen bonding (NHB) analytes. Figure 3.5 shows the log of retention factor

(k') of thirteen different analytes using OALS and SDS as the pseudostationary phase. The retention factors of OALS and SDS are strongly correlated, giving an R^2 value of 0.85 for the thirteen analytes in Figure 3.5. OALS also shows similar selectivity with SDS for HBD, HBA and NHB analytes. The R^2 of each type of interaction between OALS and SDS are 0.93, 0.99 and 0.91 for HBD, NHB and HBA class compounds respectively. The slopes and elevations of the HBD, NHB and HBA lines are compared with each other using the statistical method outlined by Zar [30]. Each line is statistically different from each other. The high R^2 values between each line are not surprising because the primary driving force between micelle and solute interaction is the hydrophobic interaction [23, 31]. However, Figure 3.5 also shows three distinct lines that indicate there is a difference in migration pattern for different classes of solutes. The difference in the migration pattern is illustrated in Figure 3.6 where the phenol and resorcinol switch places when using OALS and SDS. Sodium *N*-lauroyl-*N*-methyltaurate (LMT) has also been observed to exhibit such selectivity reversal versus SDS [32]. Like OALS, LMT has a different palisade region than SDS. This illustrates the unique selectivity of OALS compared to the SDS.

ALS and OALS have similar structures. Both contain a ketal linkage in their palisade region. The log of k' of thirteen analytes using OALS and ALS in Figure 3.7 reveals that they show very similar selectivity for individual type of analyte. The correlation coefficient between the log k' of OALS and ALS are 0.94, 0.95 and 0.98 for HBD, NHB and HBA class compounds respectively. OALS has a more similar selectivity with ALS than with SDS.

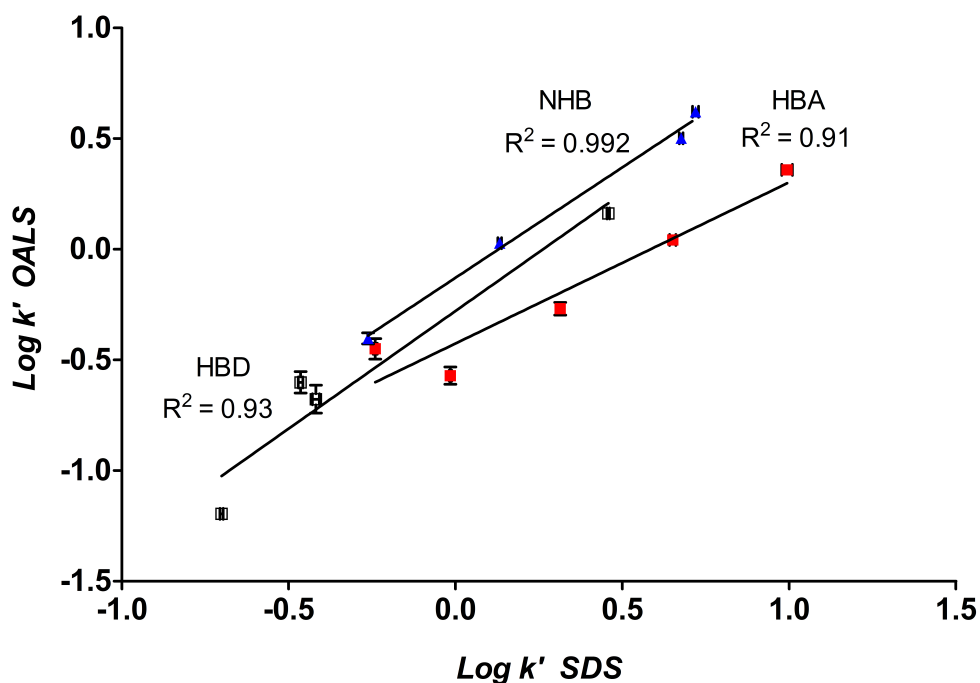


Figure 3.5 Log k' of thirteen analytes using OALS and SDS as pseudostationary phase. \square = hydrogen bond donor (resorcinol, phenol, aniline, 2-naphthol), $R^2 = 0.93$; \blacksquare = hydrogen bond acceptor (4-nitroaniline, acetophenone, propiophenone, butyrophenone, valerophenone), $R^2 = 0.91$; \blacktriangle = non-hydrogen bonding (benzene, toluene, naphthalene, 2-methylnaphthalene), $R^2 = 0.992$. Analytes are listed in order of their retention with SDS. Conditions: EOF marker, methanol; detection, 214 nm; applied voltage, 15 kV; BGE, 50 mM ammonium acetate, 30 mM OALS or SDS, pH 9.00.

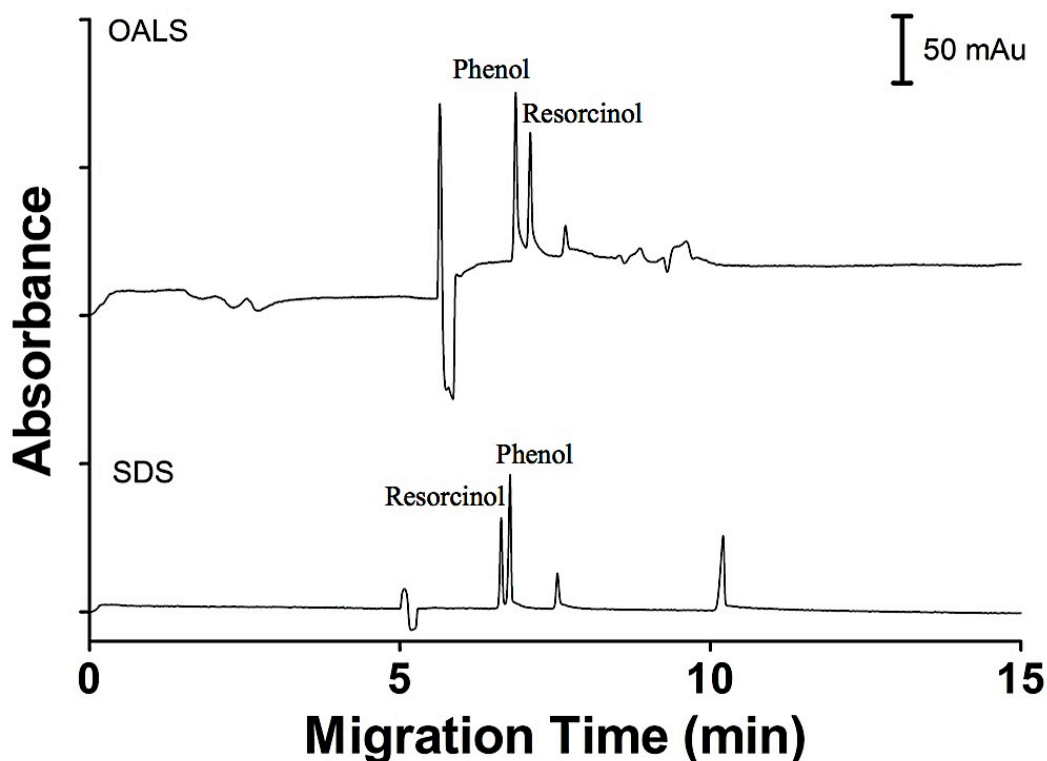


Figure 3.6 Electropherogram illustrating the difference in migration pattern of resorcinol and phenol when using OALS and SDS as pseudostationary phases. Condition: detection, 214 nm; applied voltage, 15 kV; BGE, 50 mM ammonium acetate, 30 mM OALS or SDS, pH 9.00; capillary (50 μ m ID) total length, 51.5 cm; effective length, 41.5 cm.

OALS gives separation efficiency of 105,000 – 175,000 plates for the thirteen analytes. For the same analytes, SDS achieved 125,000 – 185,000 plates and ALS displayed 75,000 – 130,000 plates. Thus, OALS performs better than ALS and comparable to SDS as a pseudostationary phase in term of separation efficiency.

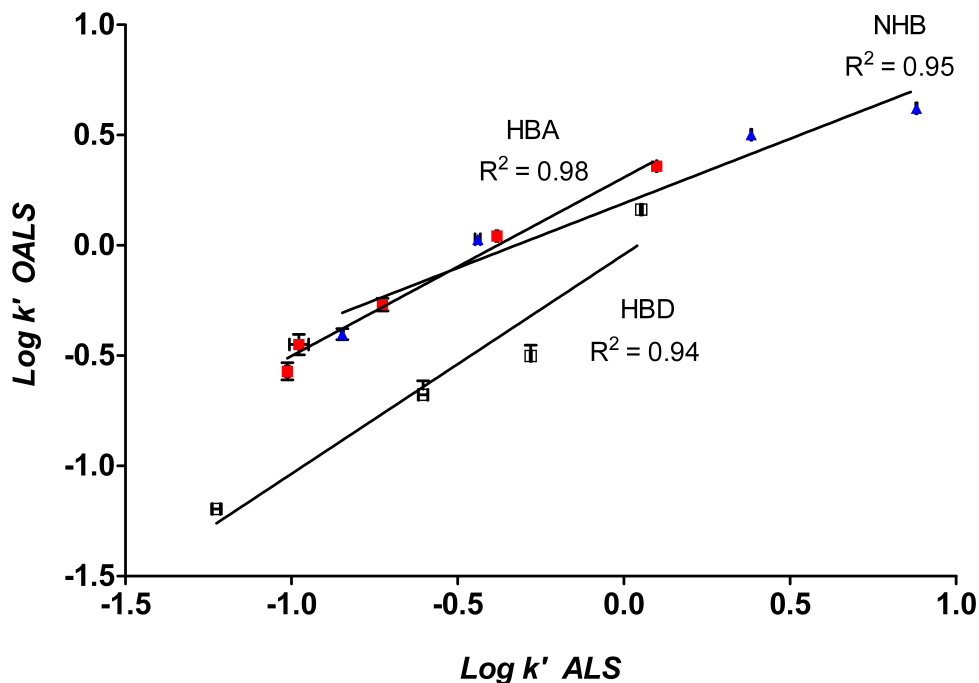


Figure 3.7 Log k' of thirteen analytes using OALS and ALS as pseudostationary phase. \square = hydrogen bond donor (resorcinol, phenol, aniline, 2-naphthol), $R^2 = 0.94$; \blacksquare = hydrogen bond acceptor (4-nitroaniline, acetophenone, propiophenone, butyrophenone, valerophenone), $R^2 = 0.98$; \blacktriangle = non-hydrogen bonding (benzene, toluene, naphthalene, 2-methylnaphthalene), $R^2 = 0.95$. Analytes are listed in order of their retention in ALS. Conditions: EOF marker, methanol; detection, 214 nm; applied voltage, 15 kV; BGE, 50 mM ammonium acetate, 30 mM OALS or SDS, pH 9.00.

3.3.2 Cleavage Rate and Compatibility with ESI-MS

OALS needs to fulfill two important criteria before it can be used to hyphenate MEKC with ESI-MS online. The acid-hydrolysis products of OALS must not be surface-active and the hydrolysis rate has to be as rapid as possible. Previously it was determined that the acid-labile surfactant, ALS has a hydrolysis half-life of 48 minutes in 0.5% formic acid (pH 2.50) and this is not fast enough to couple the MEKC with ESI-MS online [19]. As mentioned in Section 3.1, ALS contains a cyclic ketal linkage. In contrast, OALS that has an acyclic ketal linkage

are known to hydrolyze faster than cyclic ketals [20, 21]. Indeed, O'Doherty and co-workers report that OALS is completely hydrolyzed at pH 2.00 within ten minutes [22].

To monitor the rate of OALS hydrolysis, the ESI-MS signal of the model analyte tryptophan as a model analyte was monitored against the signal of OALS in the negative mode. Atenolol is used in the kinetic study of ALS (Section 2.3.4). However, the atenolol signal is suppressed by OALS even after the hydrolysis. Equimolar atenolol and tryptophan were analyzed by ESI-MS to compare the intensity of their respective signals. As shown in Figure 3.8, the tryptophan signal (m/z 203.0) is much stronger than the atenolol signal (m/z 311.2) in the negative mode. Figure 3.9 shows the presence of an intense peak at m/z 153.0. This intense peak is one of OALS hydrolysis products, i.e. the ketone (see Fig. 3.1). Initially, the atenolol peak is suppressed by OALS. After the hydrolysis of OALS, the ketone peak (m/z 153.0) dominates the atenolol peak. The tryptophan signal is still strong despite the presence of the ketone peak. Therefore, tryptophan is used as the internal standard instead of atenolol for monitoring OALS hydrolysis.

The m/z of tryptophan (203.0) is easily resolved from that of OALS (339.2). Figure 3.9 shows both the tryptophan and the OALS signals at 0 and 7 minutes after addition of 0.5% formic acid. Prior to the hydrolysis (time = 0), the OALS signal is strong and dominates the ESI signal of an equimolar solution of OALS and tryptophan. As OALS is hydrolyzed, the tryptophan signal increases while the OALS signal diminishes. As a control, the same experiment using SDS (m/z = 265.2) showed that the SDS signal still suppresses the tryptophan signal

after 30 minutes. To quantify the hydrolysis kinetics, the ESI-MS signal intensity ratio of OALS over tryptophan was plotted vs. time in Figure 3.10. The half-life of OALS at pH 2.5 is 48 ± 6 s, approximately 60 fold faster than ALS, consistent with the expected kinetics of acyclic ketal vs. its cyclic counterpart [20, 21]. Figure 3.9 shows that one of the hydrolysis products of OALS at m/z 153.0 gives a fairly intense signal. While OALS hydrolysis causes a significant improvement of tryptophan signal, the presence of the strong signal at m/z 153.0 can potentially cause ion suppression for analyte ion that gives weaker signal such as atenolol.

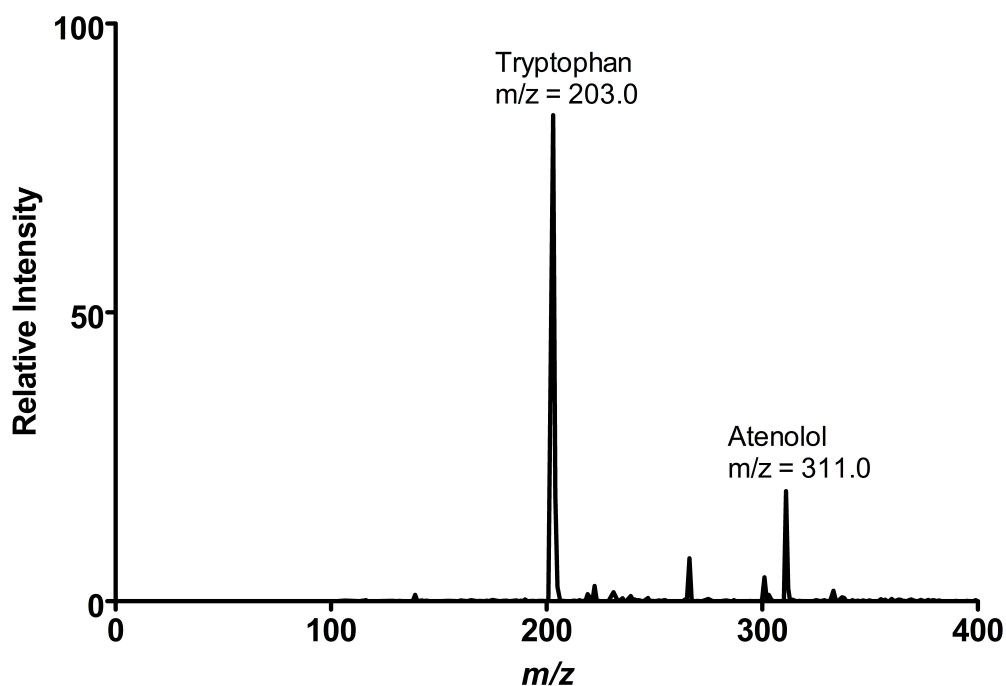


Figure 3.8 Mass spectra of equimolar tryptophan and atenolol. Conditions: 500 μ L of tryptophan (25 mM in 0.5% formic acid) and 500 μ L of atenolol (25 mM in 0.5% formic acid). Conditions: negative mode; fragmentation energy, 80 V; solvent system, methanol. Tryptophan peak is $[M-H]^-$. Atenolol peak is $[M+FA-H]^-$.

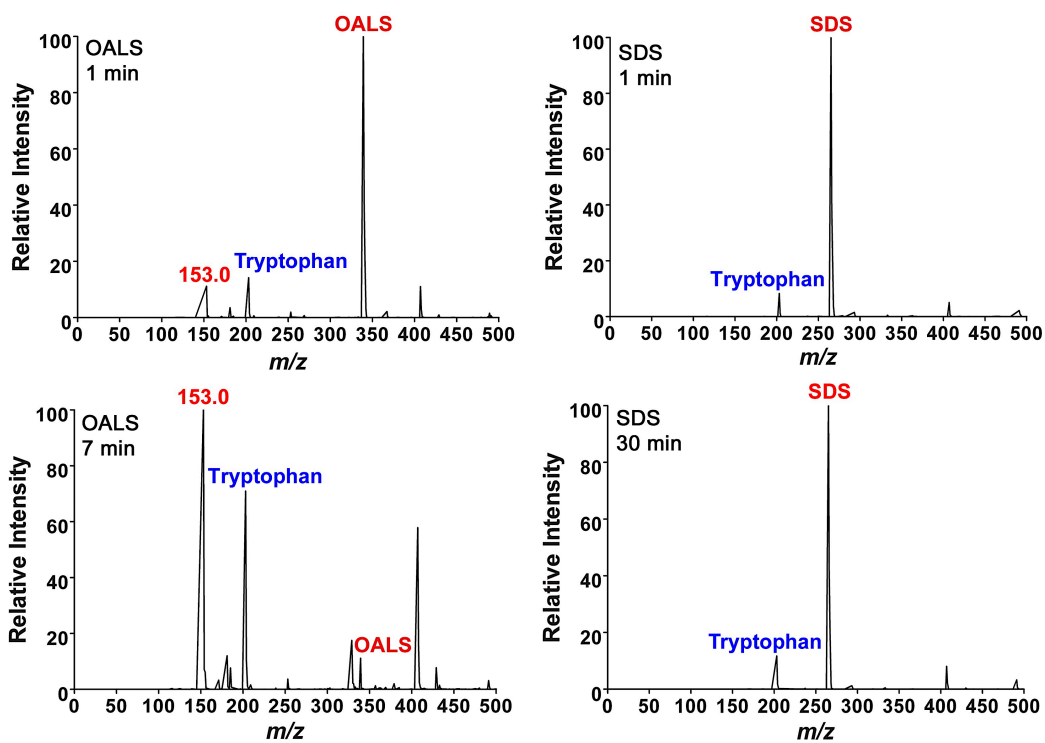


Figure 3.9 Mass spectra of tryptophan and OALS at 0 minute and 7 minute. Mass spectra of SDS at 1 and 30 minute as control. Conditions: 475 μL of tryptophan (25 mM in 0.5% formic acid) spiked with 25 μL of OALS (25 mM in deionized water). Conditions: negative mode; fragmentation energy, 80 V; solvent system, methanol. Tryptophan peak is $[\text{M}-\text{H}]^-$. OALS peak is $[\text{M}]^-$.

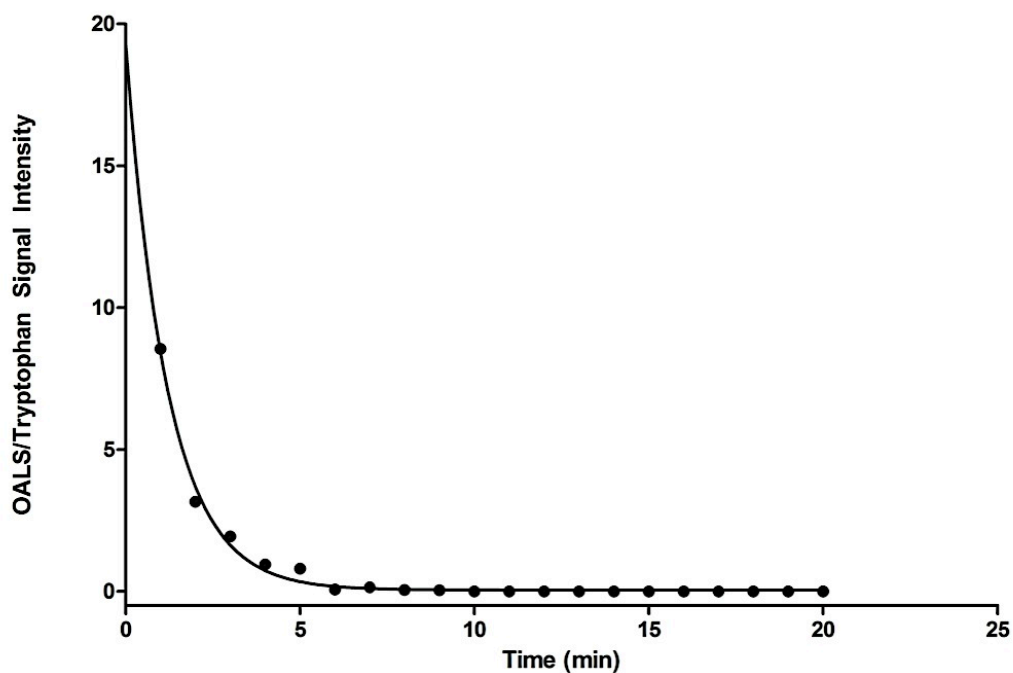


Figure 3.10 Ratio of OALS/tryptophan ESI-MS signal intensity over a period of 20 minutes in H₂O. Conditions: 475 μ L of tryptophan (25 mM in 0.5% formic acid), pH 2.5, spiked with 25 μ L of OALS (25 mM in deionized water). Conditions: fragmentation energy, 80 V; solvent system, methanol; Half-life of OALS, 48 s.

Low molecular weight surfactants such as SDS completely suppress the analyte ion signal in an ESI positive ion mode [33-35]. Figure 3.11 shows the tryptophan signal ($m/z = 205.0$) in a positive mode in the presence of OALS at 1 and 3 min after addition of 0.5% formic acid. At 1 minute, much of the OALS remains intact, such that the tryptophan signal in positive ESI is suppressed (relative intensity = 49). However, by 3 min (~ 3.8 half lives), the tryptophan

signal is back at relative intensity = 100. This clearly shows the compatibility of OALS after hydrolysis with ESI-MS in a positive ion mode.

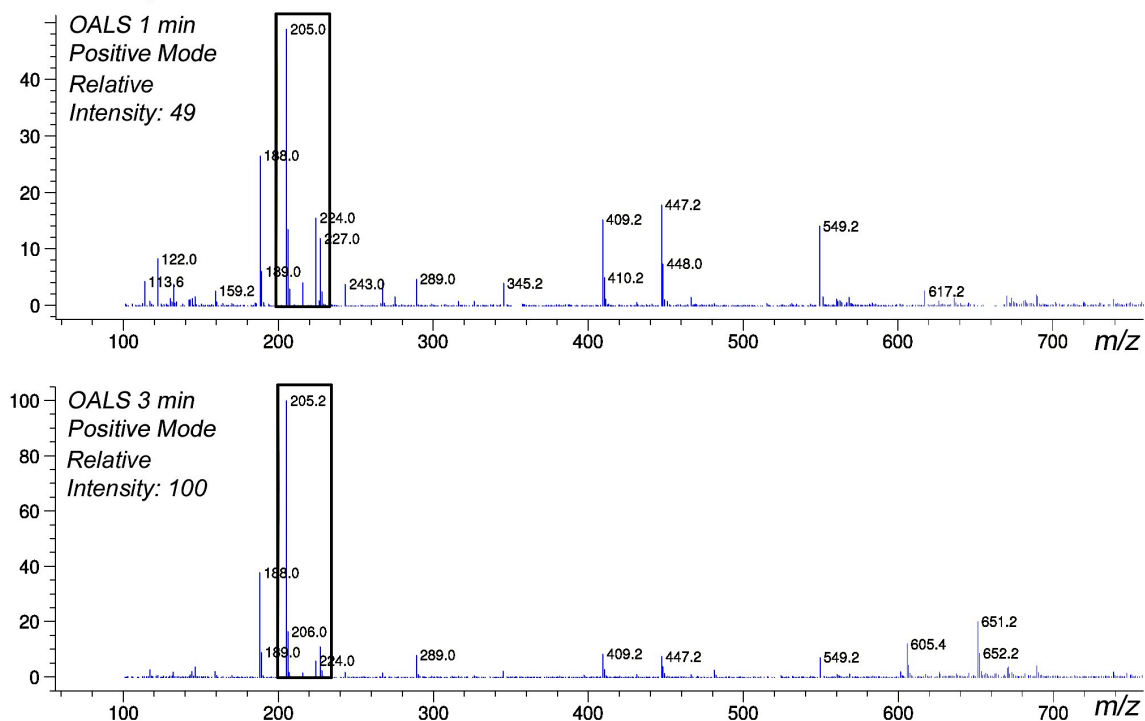


Figure 3.11 Tryptophan ESI-MS positive ion signal intensity ($m/z = 205.0$) over a period of 3 minutes in H_2O in a presence of OALS. Conditions: $475 \mu L$ of tryptophan (25 mM in 0.5% formic acid), pH 2.5, spiked with $25 \mu L$ of OALS (25 mM in deionized water). Conditions: fragmentation energy, 80 V; solvent system, methanol.

3.3.3 Controlling the Hydrolysis Rate of OALS with Temperature

MEKC separations normally take between 5 – 15 minutes and can be much longer [8, 31]. It is necessary that OALS be stable during the MEKC, and then rapidly hydrolyzed after the separation is finished. A way to achieve this is by using temperature. Reaction rate is dependent on the temperature of the

reaction [36]. The hydrolysis of OALS should not be any different. To monitor the effect of temperature on the hydrolysis rate of OALS, the signal of OALS and tryptophan in an equimolar solution (pH 2.5) was monitored at 4 °C. OALS degrades readily under the same condition at room temperature, 21 °C (see Fig 3.10). The ratio of OALS and tryptophan signal is plotted vs. time (min). Figure 3.12 shows that there is no visible degradation of OALS within 20 min. The slope of the line (0.012 ± 0.08) is statistically equal to 0 at the 95% confidence limit. The plot shows that lowering the temperature slows down the hydrolysis rate of OALS. However, the relative standard deviation (RSD) of the data is 28%, which is fairly significant. At 4°C, most of the OALS is not hydrolyzed. A high concentration of anionic surfactant destabilizes the Taylor cone [18, 37, 38]. This results in inconsistent ESI nebulization resulting in the high RSD.

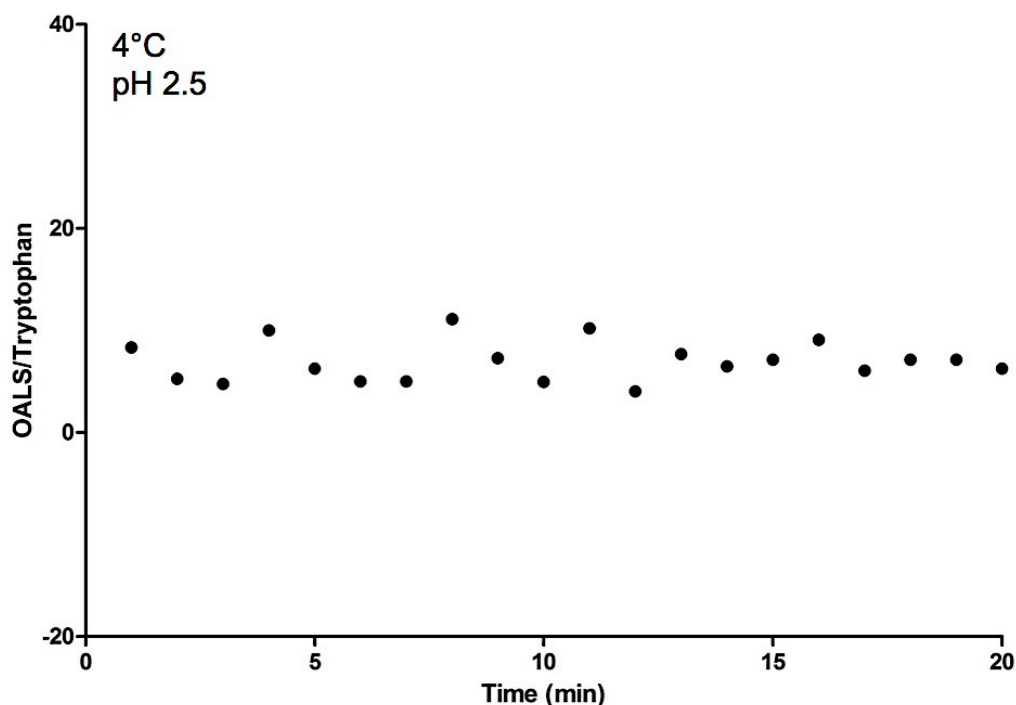


Figure 3.12 Ratio of OALS/tryptophan ESI-MS signal intensity over a period of 20 minutes in H₂O at 4 °C. Conditions: 475 μL of tryptophan (25 mM in 0.5% formic acid), pH 2.5, spiked with 25 μL of OALS (25 mM in deionized water). Conditions: fragmentation energy, 80 V; solvent system, methanol.

If lowering the temperature slows down the hydrolysis rate of OALS, increasing the temperature must speed up the hydrolysis of OALS. The half-life of OALS at pH 2.5 is very rapid (48 ± 6 s) at room temperature (21 °C), and so it would be difficult to monitor the hydrolysis at pH 2.5 with our current apparatus. MEKC experiments are typically performed at higher pH. Therefore, the effect of temperature on the hydrolysis rate was performed at pH 4.50. At 21°C, the rate constant of OALS hydrolysis at pH 4.50 is close to 4 orders of magnitude smaller than that at pH 2.50. Thus, if an MEKC separation were performed at pH 4.50 (21 °C), the OALS would be intact throughout the separation, but its presence would then suppress the ESI.

Figure 3.13 shows the hydrolysis rate of OALS at pH 4.50 at 21 and 60 °C. The OALS hydrolysis rate is slow at 21 °C. However, when the temperature is increased to 60 °C, the hydrolysis rate of the OALS is much faster. The rate constant of the hydrolysis from 21 °C to 60 °C increases 3 order of magnitude. This is consistent with the concept that as temperature is increased, the hydrolysis rate speeds up.

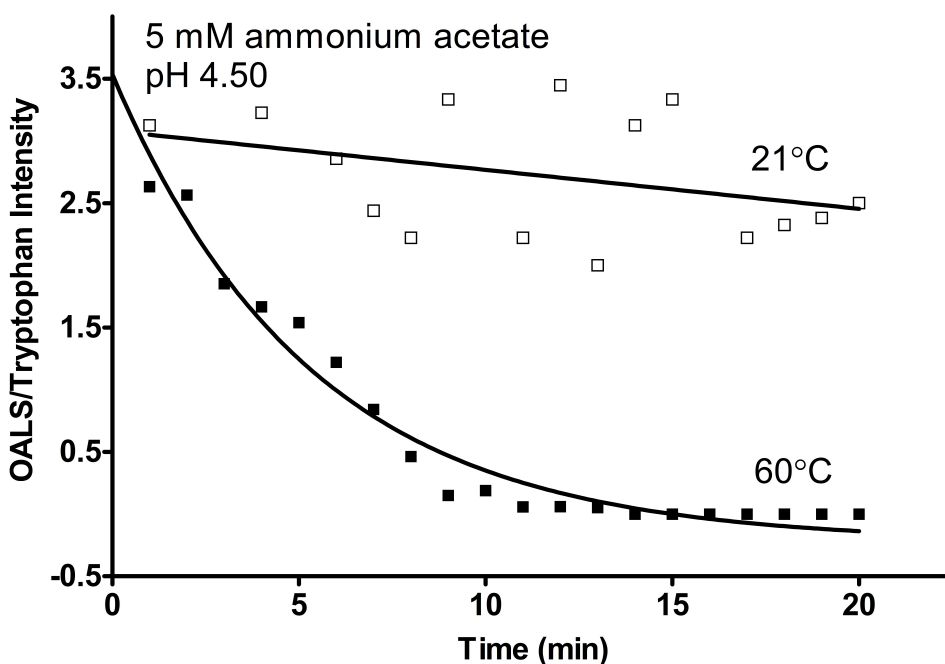


Figure 3.13 Ratio of OALS/atenolol ESI-MS signal intensity at 21°C and 60°C over a period of 20 minutes in H₂O showing an increase in the rate constant of OALS hydrolysis as temperature is increased. Conditions: 475 µL of tryptophan (5 mM ammonium acetate), pH 4.50, spiked with 25 µL of OALS (25 mM in deionized water). Conditions: fragmentation energy, 80 V; solvent system, methanol

The commercial capillary electrophoresis (CE) instrument can control the capillary temperature in any range between 20 – 60 °C. Based on Fig. 3.13, it should be possible to perform an MEKC separation using OALS at room temperature and pH 4.50, then stop the applied voltage, increase the capillary

temperature to 60 °C to hydrolyze the OALS and finally re-apply the voltage to deliver the separated analytes into an on-line ESI-MS. To test this hypothesis, a fresh pH 4.50 30 mM OALS solution was prepared and an MEKC separation was performed at a capillary temperature of 21 °C. Figure 3.14 shows the MEKC separation at 21 °C. The OALS should not be rapidly hydrolyzed under this condition and the neutral analytes should be separated. The model neutral analytes phenol, resorcinol and 4-nitroaniline are separated with an efficiency of 120,000 – 160,000 plates which is comparable with SDS, but higher than ALS. The peak that comes out before 4-nitroaniline is an impurity.

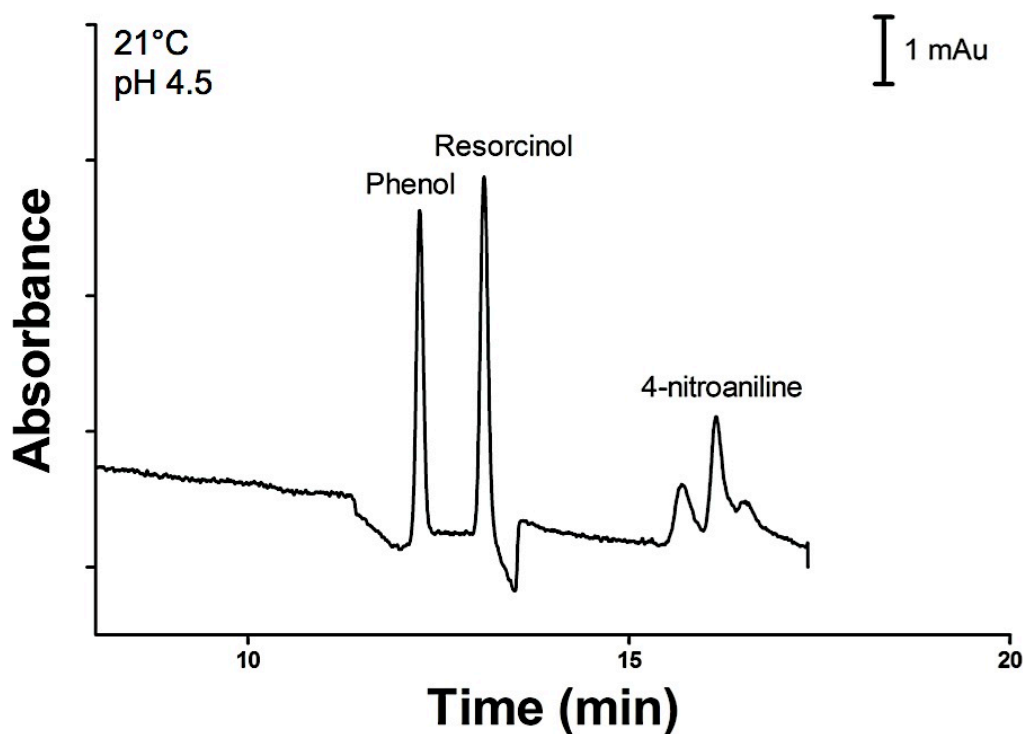


Figure 3.14 Electropherogram of separation of phenol, resorcinol and 4-nitroaniline at 21 °C showing that OALS has not been hydrolyzed. Condition: detection, 214 nm; applied voltage, 15 kV; BGE, 5 mM ammonium acetate, 30 mM OALS, pH 4.50; capillary (50 μ m ID) total length, 51.5 cm; effective length, 41.5 cm.

A fresh pH 4.50 30 mM OALS solution is prepared and the experiment is repeated, but this time at 60 °C. According to the ESI-MS experiment (Fig. 3.12), a good portion of the OALS should have been degraded after 216 s. The separation of the three neutral analytes would suffer. Figure 3.14 shows that the resolution has significantly decreased. The analysis time has also decreased. OALS is an anionic surfactant and its micelle travels against the EOF. When OALS is hydrolyzed, the EOF is more dominant and there are fewer amounts of micelles available. When there are fewer amounts of micelles, the analytes on average spend more time in the bulk solution and reach the detector faster [39]. This experiment supports the ESI-MS experiment in showing that temperature can be used to control the hydrolysis rate of OALS prior to its introduction to the ESI-MS.

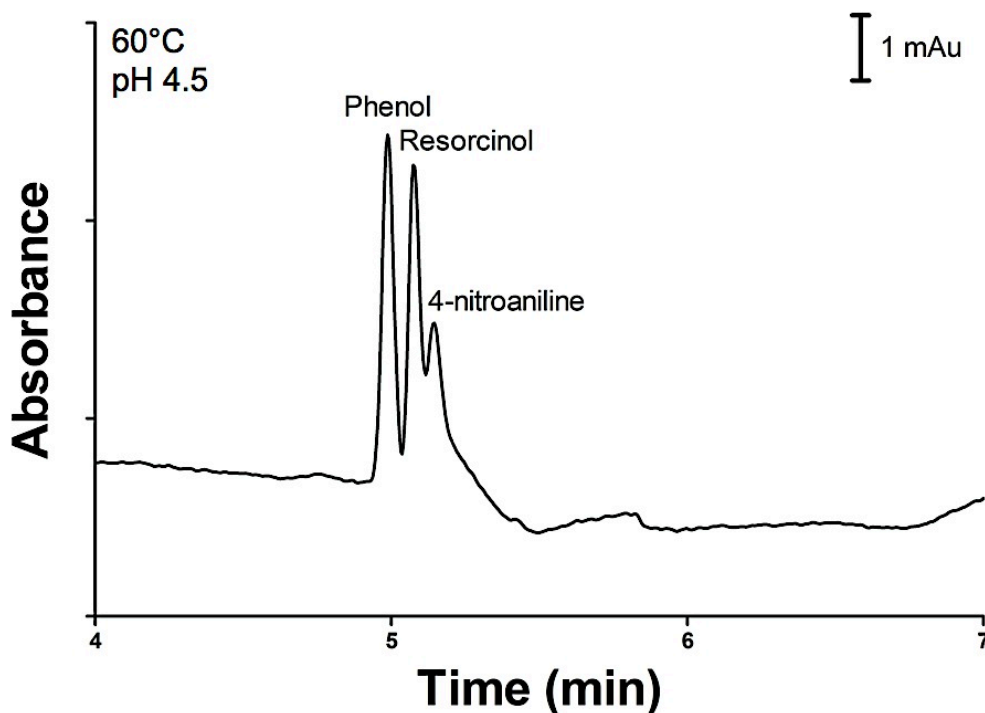


Figure 3.15 Electropherogram of separation of phenol, resorcinol and 4-nitroaniline at 60 °C showing that a good portion of OALS has been hydrolyzed. Condition: detection, 214 nm; applied voltage, 15 kV; BGE, 5 mM ammonium acetate, 30 mM OALS, pH 4.50; capillary (50 μm ID) total length, 51.5 cm; effective length, 41.5 cm.

3.4 CONCLUDING REMARKS

Sodium 2,2-Bis(hexyloxy)propyl sulphate (OALS) is a surfactant with an acyclic ketal linkage. OALS offers unique selectivity compared to SDS. However, it has similar selectivity compared with sodium 4-[(2-methyl-2-undecyl-1,3-dioxolan-4-yl) methoxy]-1-propane sulfonate (ALS). OALS also has the fastest mobility compared to SDS and ALS, which results in OALS giving the largest migration time window (t_{mc}/t_{eof}). The acyclic ketal linkage in OALS is more labile than its cyclic counterpart. Thus, OALS has a much faster hydrolysis rate compared to ALS. Varying the temperature can control this fast hydrolysis rate.

Temperature can be used to slow down the hydrolysis rate, allowing the use of OALS in MEKC separation. Once the separation is finished, the temperature can be raised to speed up the hydrolysis rate of OALS before introducing the analyte into the ESI-MS. The hydrolysis product of OALS is compatible with ESI-MS.

3.5 REFERENCES

- [1] J.B. Fenn, M. Mann, C.K. Meng, S.F. Wong, C.M. Whitehouse, *Science*, 246 (1989) 64.
- [2] J.B. Fenn, M. Mann, C.K. Meng, S.F. Wong, C.M. Whitehouse, *Mass Spectrom. Rev.*, 9 (1990) 37.
- [3] R.D. Smith, J.A. Loo, C.G. Edmonds, C.J. Barinaga, H.R. Udseth, *Anal. Chem.*, 62 (1990) 882.
- [4] T.M. Annesley, *Clinical Chemistry*, 49 (2003) 1041.
- [5] R. King, R. Bonfiglio, C. Fernandez-Metzler, C. Miller-Stein, T. Olah, *J. Am. Soc. Mass Spectrom.*, 11 (2000) 942.
- [6] S. Terabe, K. Otsuka, K. Ichikawa, A. Tsuchiya, T. Ando, *Anal. Chem.*, 56 (1984) 111.
- [7] S. Terabe, K. Otsuka, T. Ando, *Anal. Chem.*, 57 (1985) 834.
- [8] S. Terabe, *Chem. Rec.*, 8 (2008) 291.
- [9] S. Terabe, *Annu. Rev. Anal. Chem.*, 2 (2009) 99.
- [10] M. Silva, *Electrophoresis*, 32 (2011) 149.
- [11] P. Ladarola, F. Ferrari, M. Furnagalli, S. Viglio, *Electrophoresis*, 29 (2008) 224.
- [12] H. Schwaiger, P.J. Oefner, C. Huber, E. Grill, G.K. Bonn, *Electrophoresis*, 15 (1994) 941.
- [13] B. Stanley, K.A. Mehr, T. Kellock, J.D. Van Hamme, K.K. Donkor, *J. Sep. Sci.*, 32 (2009) 2993.
- [14] V. Kasicka, *Electrophoresis*, 33 (2012) 48.

- [15] M. Silva, *Electrophoresis*, 28 (2007) 174.
- [16] C.W. Klampfl, *Electrophoresis*, 30 (2009) S83.
- [17] C.W. Klampfl, W. Buchberger, *Anal. Bioanal. Chem.*, 388 (2007) 533.
- [18] K.L. Rundlett, D.W. Armstrong, *Anal. Chem.*, 68 (1996) 3493.
- [19] B. Stanley, C.A. Lucy, *J. Chromatogr. A*, 1226 (2012) 55.
- [20] E.H. Cordes, H.G. Bull, *Chem. Rev.*, 74 (1974) 581.
- [21] P. Deslongchamps, Y.L. Dory, S. Li, *Tetrahedron*, 56 (2000) 3533.
- [22] M.S. Li, M.J. Powell, T.T. Razunguzwa, G.A. O'Doherty, *J. Org. Chem.*, 75 (2010) 6149.
- [23] S. Yang, J.G. Bumgarner, L.F.R. Kruk, M.G. Khaledi, *J. Chromatogr. A*, 721 (1996) 323.
- [24] J.G. Bumgarner, M.G. Khaledi, *Electrophoresis*, 15 (1994) 1260.
- [25] H. Nishi, T. Fukuyama, M. Matsuo, S. Terabe, *J. Chromatogr. A*, 513 (1990) 279.
- [26] E.S. Ahuja, E.L. Little, K.R. Nielsen, J.P. Foley, *Anal. Chem.*, 67 (1995) 26.
- [27] E. Fuguet, C. Ràfols, E. Bosch, M. Rosés, *Electrophoresis*, 23 (2002) 56.
- [28] M.M. Bushey, J.W. Jorgenson, *Anal. Chem.*, 61 (1989) 491.
- [29] P.G. Muijselaar, M.A. Van Straten, H.A. Claessens, C.A. Cramers, *J. Chromatogr. A*, 766 (1997) 187.
- [30] J.J. Zar, *Biostatistical Analysis*, Prentice-Hall, Upper Saddle River, New Jersey, 2nd ed., 1984.
- [31] S. Yang, M.G. Khaledi, *Anal. Chem.*, 67 (1995) 499.

- [32] E. Nomura, K. Katsuta, T. Ueda, M. Toriyama, T. Mori, N. Inagaki, *Journal of Mass Spectrometry*, 39 (2004) 202.
- [33] J. Cai, J. Henion, *J. Chromatogr. A*, 703 (1995) 667.
- [34] W.M.A. Niessen, U.R. Tjaden, J. van der Greef, *J. Chromatogr. A*, 636 (1993) 3.
- [35] R.D. Smith, J.H. Wahl, D.R. Goodlett, S.A. Hofstadler, *Anal. Chem.*, 65 (1993) 574A.
- [36] S. Arrhenius, *Z. Physik. Chem.*, 4 (1889) 226.
- [37] J. Schappler, D. Guillarme, S. Rudaz, J.-L. Veuthey, *Electrophoresis*, 29 (2008) 11.
- [38] G.W. Somsen, R. Mol, G.J. de Jong, *J Chromatogr A*, 1000 (2003) 953.
- [39] S. Terabe, *Anal. Chem.*, 76 (2004) 240A.

CHAPTER 4

Section 4.1 GENERAL DISCUSSION AND CONCLUSIONS

The potential of the acid cleavable surfactants sodium 4-[(2-methyl-2-undecyl-1,3-dioxolan-4-yl) methoxy]-1-propane sulfonate (ALS) and sodium 2,2-Bis(hexyloxy)propyl sulphate (OALS) as pseudostationary phases for micellar electrokinetic chromatography (MEKC) have been investigated in this thesis. The selectivity and mobility of ALS and OALS are compared with the most widely used surfactant, SDS [1, 2]. ALS and OALS show unique selectivity compared to SDS. However, they show similar selectivity with each other because they contain a similar ketal-linkage. The presence of ketal-linkage in the palisade region of ALS and OALS make them hydrolyzable under acidic condition. The hydrolysis products of ALS and OALS are compatible with electrospray ionization mass spectrometry (ESI-MS).

In Chapter 2, the performance of ALS as a pseudostationary phase was compared with SDS. ALS offers a unique selectivity compared to SDS. The mobility of ALS is slower than SDS resulting in a smaller migration time window. ALS yields slightly lower separation efficiency than SDS, but ALS still gives comparable separation efficiency with other ESI-MS compatible pseudostationary phases. ALS contains a cyclic ketal linkage and degrades under acidic condition. The degradation product of ALS is compatible with ESI-MS. The half-life of ALS is 48 ± 12 minutes at pH 2.5. This half-life is too long for ALS to be used in

online MEKC-ESI-MS. However, the use of ALS in offline MEKC-ESI-MS is feasible.

The characteristics of OALS for MEKC separations and ESI-MS detection are investigated in Chapter 3 of this thesis. The selectivity and mobility of OALS are compared with ALS and SDS. OALS has a unique selectivity compared to SDS. This is illustrated in Figure 3.5 where phenol and resorcinol switch places when using SDS and OALS as pseudostationary phases. OALS shares a similar ketal-linkage with ALS and they share similar selectivity as indicated by the high correlation of the $\log k'$ plot of Figure 3.6. OALS has greater mobility than SDS and ALS resulting in a wider migration time window, and hence larger peak capacity. OALS contains an acyclic ketal-linkage, which is more labile than the cyclic ketal-linkage of ALS. Therefore, OALS degrades much faster than ALS under the same acidic condition. The half-life of OALS is 48 ± 6 s at pH 2.5. Unfortunately, one of the hydrolysis products of OALS gives an intense signal. This intense signal does not suppress an analyte ion signal as badly as OALS. However, it causes some ion suppression as evident in suppression of the atenolol signal. Varying the temperature can control the hydrolysis rate of OALS. Lowering the temperature slows down the hydrolysis rate and vice versa. This allows the use of OALS in an MEKC separation, hydrolyze it by increasing the temperature and introduce the separated analytes conveniently into the ESI-MS.

Section 4.2 FUTURE WORK

Ketal-containing surfactants such as ALS and OALS are a possible bridge to hyphenate MEKC with ESI-MS. The faster hydrolysis rate of OALS is attractive for on-line ESI-MS. It is proposed that the hydrolysis rate of OALS could be accelerated even more by introducing an electron-donating group such as a dimethyl group to the carbon right next to the ketal oxygen. The rate-determining step of a ketal hydrolysis is the protonation of the ketal oxygen. Introducing an electron-donating group such as a dimethyl group to the carbon next to the oxygen would increase the electron density around the oxygen. This should make the oxygen more readily protonated resulting in faster hydrolysis. However, enhancing the hydrolysis rate would not address my key concerns with OALS – that its hydrolysis products interfere with negative mode ESI-MS.

ALS has been used previously as a substitute for SDS in polyacrylamide gel electrophoresis (PAGE) of peptides and proteins because ALS has a similar denaturing and electrophoretic properties [3, 4]. OALS has not been applied in PAGE of peptides and proteins. The use of OALS in PAGE of peptides and proteins can become a significant scientific contribution in the field of proteomics.

An excellent candidate for enabling the combination of MEKC and ESI-MS would be a magnetic surfactant [5]. A magnetic surfactant is a surfactant that is responsive to a magnetic field. The magnetic surfactant can be used as a pseudostationary phase for an MEKC separation and the prevented from being introduced to the ESI-MS by a magnetic field.

In summary, the combination of MEKC with ESI-MS is very attractive because that will harness the high efficiency separation power of MEKC and the versatility of ESI-MS. The hyphenation is fraught with challenges, but it is not an impossible task. The hybridization of both techniques is going to provide the scientific community with an additional formidable analytical methodology.

4.3 REFERENCES

- [1] S. Terabe, *Annu. Rev. Anal. Chem.*, 2 (2009) 99.
- [2] M. Silva, *Electrophoresis*, 32 (2011) 149.
- [3] S. Konig, O. Schmidt, K. Rose, S. Thanos, M. Besselmann, M. Zeller, *Electrophoresis*, 24 (2003) 751.
- [4] E. Nomura, K. Katsuta, T. Ueda, M. Toriyama, T. Mori, N. Inagaki, *Journal of Mass Spectrometry*, 39 (2004) 202.
- [5] P. Brown, A. Bushmelev, C.P. Butts, J. Cheng, J. Eastoe, I. Grillo, R.K. Heenan, A.M. Schmidt, *Angew. Chem. Int. Ed. Engl.*, (2012) 1.